AD-A059 855 ENVIRONMENTAL RESEARCH INST OF MICHIGAN ANN ARBOR RA--ETC F/G 17/8
INVESTIGATIONS OF A GOGGLE DESIGN UTILIZING HOLOGRAPHIC OPTICS.(U)
SEP 75 W S COLBURN DAAK02-75-C-0056
UNCLASSIFIED ERIM-112200-1-T NL

1 OF 1
AD
A059855

END
DATE
FILMED
12-78
DDC

AD A059855
112200-1-T

DDC FILE COPY

AD ______

LEVEL II

Interim Technical Report

INVESTIGATIONS OF A GOGGLE DESIGN UTILIZING HOLOGRAPHIC OPTICS

WILLIS S. COLBURN
Radar and Optics Division

SEPTEMBER 1975

Approved for Public Release;
Distribution Unlimited

Night Vision Laboratory
U.S. Army Electronics Command
Fort Belvoir, Virginia 22060

Contract No. DAAK02-75-C-0056

ENVIRONMENTAL RESEARCH INSTITUTE OF MICHIGAN
FORMERLY WILLOW RUN LABORATORIES, THE UNIVERSITY OF MICHIGAN
BOX 618 • ANN ARBOR • MICHIGAN 48107

78 10 05 016

14

ERIM-112200-1-T

AD ____________

6 INVESTIGATIONS OF A GOGGLE DESIGN UTILIZING HOLOGRAPHIC OPTICS.

9 Interim Technical Report.
6 Nov 74-6 Mar 75,

10 by
Willis S. Colburn
Radar and Optics Division
Environmental Research Institute of Michigan
P. O. Box 618, Ann Arbor, Michigan 48107

May 1975

for
Night Vision Laboratory
U.S. Army Electronics Command
Fort Belvoir, Virginia 22060

15
Contract No. DAAK02-75-C-0056
DA Project/Task Number
16 1S763719DK70 13 17

Distribution Unlimited

11 Sep 75 12 86p.

ABSTRACT

SUMMARY

This report covers a preliminary design effort to develop a one-tube, two-eye goggle utilizing holographic optical elements. The major objective of this effort was to determine the feasibility of using holographic optics in a goggle system with its requirements of wide field-of-view, high efficiency, and good image quality. Because of the dispersive nature of holograms, holographic lenses operate best over a narrow band of wavelengths; for the night glass application, therefore, holographic elements were considered only for the portion of the optical train following the image intensifier. In the course of this design effort, nine variations of a basic system configuration were evaluated in terms of imaging criteria, aberrations, and efficiency. Two designs showed promise, although further improvements are necessary. One design is all-holographic and offers a minimum of complexity, but appears to require new techniques to achieve the required performance levels. The second promising design included two hologram lenses and two conventional lenses (for each eye) but was more complex than the all-holographic system.

ABSTRACT

FOREWORD

This report was prepared by the Radar and Optics Division of the Environmental Research Institute of Michigan. The work was sponsored by the Night Vision Laboratory under Contract No. DAAK02-75-C-0056.

This interim report covers work performed between 6 November 1974 and 6 March 1975. The contract monitor is Mr. Jasper C. Lupo, Visionics Technical Area, Night Vision Laboratory. The principal investigator is W. S. Colburn. Major contributors to the effort are W. S. Colburn and J. N. Latta.

TABLE OF CONTENTS

TABLE OF CONTENTS
(continued)

LIST OF ILLUSTRATIONS

LIST OF ILLUSTRATIONS
(continued)

LIST OF TABLES

1
INTRODUCTION

This report covers a preliminary effort to develop a one-tube, two-eye goggle design utilizing holographic optical elements. Holographic optics offers the potential of elements that are lightweight and easily replicated in production quantities. The major objective of this effort was to determine the feasibility of using holographic optics in an application where the requirements of wide field-of-view, high efficiency, and good resolution together place severe demands on the hologram performance.

Holographic lenses interact with light through diffractive processes rather than the refractive or reflective processes of conventional optics. Although they may be formed on substrates of any shape, holograms are usually recorded on thin, flat substrates so that holographic lenses tend to be lightweight and thin. In addition the lenses may be recorded for use in either reflection or transmission configurations depending on the requirements of the desired application. Since holograms are formed by a photographic type of process, once the construction apparatus has been assembled, fabrication of holographic elements is rapid and relatively simple.

Furthermore, holograms in general can be replicated by photographic processes similar to contact copying so that production of holographic lenses can be carried out easily and at low cost.

Unlike most conventional optical elements, holographic elements generally do not possess rotational symmetry. Consequently the analysis of optical systems that include holographic elements requires some care. A paraxial analysis developed by Champagne [1] can be used for a first order approach in laying out the basic system design. The results presented herein were obtained with the Holographic Optics Analysis and Design ray-tracing programs developed by Latta [2-5]. These programs make possible the rapid

1. E.B. Champagne, "A Qualitative and Quantitative Study of Holographic Imaging," (unpublished PhD dissertation), Ohio State University, Columbus, 1967 (University Microfilms No. 67-10876).

2. J. N. Latta, "Computer-Based Analysis of Holography," PhD Thesis, University of Kansas, Lawrence, Kansas, December 1970 (University Microfilms No. 71-27,168).

3. J.N. Latta, "Computer-Based Analysis of Hologram Imagery and Aberrations," Appl. Opt., 10, pp. 599-618, March 1971.

4. J.N. Latta, "Computer-Based Analysis of Holography Using Ray Tracing," Appl. Opt., 10, pp. 2698-2710, Dec. 1971.

5. J.N. Latta and R.C. Fairchild, "New Developments in the Design of Holographic Optics," Proc. of Seminar on Applications of Geometrical Optics (W.J. Smith, ED), Society of Photo-Optical Instrumentation Engineers, Redondo Beach, 1973, pp. 107-126.

analysis of complex optical systems comprised of combinations of holograms, lenses, and apertures, and permit the designer to modify system parameters quickly and easily.

Conventional optical elements in general refract or reflect most of the incident light into the desired image. Holograms, on the other hand, must be of the proper type and recorded with the proper exposure parameters to form an image with high efficiency[6-7]. Thus, it is necessary to carefully select the hologram type and recording parameters, and even in a design effort, to give some consideration to the existence and availability of suitable recording materials.

Finally, because holographic lenses are diffractive by nature, they tend to perform best when used with single-frequency or narrow-band illumination. Although achromatization techniques are available,[8-10] they generally add

---

6. H. Kogelnik, in Proceedings of Symposium on Modern Optics, J. Fox, Ed, (Polytechnic Press, Brooklyn, NY, 1967) pp. 605-617.
7. W. S. Colburn, R. G. Zech, and L.M. Ralston, "Holographic Optical Elements," Technical Report, AFAL-TR-72-409 (1973).
8. J.N. Latta, "Analysis of Multiple Hologram Optical Elements with Low Dispersion and Low Aberrations," Appl. Opt, 11, pp. 1686-1696, Aug. 1972.
9. H.W. Rose, "Holographic Lens Systems," PhD Thesis, Dept. of Electrical Engrg. Ohio Stat Univ., Col. Ohio, 1972.
10. R.H. Katyl, "Compensating Optical Systems, Part I: Broadband Holographic Reconstruction," Appl. Opt, 11, pp. 1241-1247, May 1972.

considerable complexity to the system in the form of additional elements and constraints.

2
OBJECTIVES

The objective of this research effort was to design a one-tube, two-eye goggle utilizing holographic optical elements. Holographic optics are attractive for this application because of their low weight and their low potential cost (in production). In addition, they have certain unique properties, most useful of which to this effort is the ability to behave simultaneously as both a beamsplitter and a lens. Because holographic optics perform best with narrow band or single wavelength illumination, the design was limited to the portion of the optical train following the image intensifier of the goggle, where the illumination bandwidth is limited to that of the intensifier phosphor.

The basic configuration assumed for the goggle design is shown schematically in Figure 1. The dual objective lens and image intensifier tube of the present goggle is replaced by a single objective and intensifier, located on the centerline between the eyes. Because of the very broad spectrum of the radiation incident to the image intensifier, we retain the conventional objective lens. The input to the holographic optics is therefore the phosphor output of the intensifier tube.

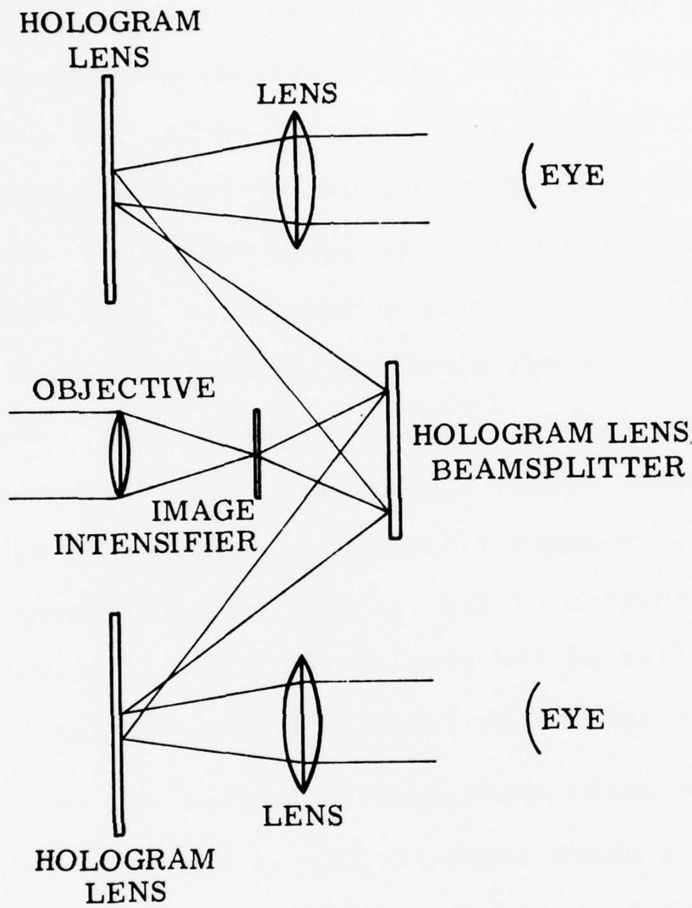

FIGURE 1. SCHEMATIC CONFIGURATION OF ONE-TUBE, TWO-EYE NIGHT GLASS WITH HOLOGRAPHIC OPTICAL ELEMENTS

Because the objective lens forms an inverted image at the intensifier, it is necessary to re-invert the image in the optics following the phosphor screen. In the present goggle, inversion is accomplished with a fiber-optics twist. Although it is a clever means of providing image inversion in a very short distance, the twist adds considerable weight to the system, a serious disadvantage. In most of our design approaches, therefore, the image is inverted by the holographic optics as shown in Figure 1.

To minimize the large cantilever effect that occurs when the optics extend far from the user's face, we chose to fold the optical path as shown in Figure 1. The first hologram element behaves as a beamsplitter as well as a lens, diverting 50% of the light towards each secondary hologram lens. To provide for image inversion the hologram lenses must have relatively short focal lengths.

In Figure 1 we show a final conventional lens between the secondary hologram and the eye. This lens completes the formation of the image and allows for an additional amount of correction in the final stages of the design.

Primary considerations in the design effort were proper imaging, high efficiency, and good image quality. The imaging conditions required that the image be formed at infinity over a 40^{o} field-of-view, and with the correct parity. The exit pupil diameter is 10 mm and eye relief is 15 mm. Efficiency goals were 50% transmission to each eye over the entire field-of-view and exit pupil. The goal for image quality was an MTF of 30% or better at a resolution of 40 ℓ/mm.

The efficiency goal of 50% transmission to each eye requires that the first hologram lens diffract 50% to each secondary lens, and that each of the latter be 100% efficient. Although the effort reported herein was purely a study effort, we point out that in practice it is reasonable to expect such performance from holograms recorded in dichromated gelatin. Indeed, we have measured diffraction efficiencies in excess of 90% for reflection holograms recorded in this material[11]. Holograms of this type are volume phase holograms; their interaction with light is in the nature of Bragg diffraction, as x-rays are diffracted by crystalline structures, and thus high efficiencies occur for preferential directions and wavelengths. Since the efficiences are high over a limited range of angles and wavelengths, therefore, it is necessary to examine the efficiency with which eacy ray is diffracted at all field angles and input wavelengths.

11. W.S. Colburn, ARPA Quarterly Technical Report on Evaluation of Hologram Optical Elements, Report No. 194500-4-T, Environmental Research Institute of Michigan, Ann Arbor, February 1974.

3

In order to study in as much detail as possible the concept of a goggle utilizing holographic optics, we decided to concentrate on the basic design shown in Figure 1. In the course of the study, however, we considered nine variations of the basic system. Figure 2 indicates the overall procedure we used in the examination of the goggle designs. Once the basic system requirements were established, in this case the imaging condition, the desired high diffraction efficiency, the wavelength region of interest, and the desired image quality, we selected several design approaches.

For each design approach, we traced rays through the system for several field angles and evaluated the system performance in terms of image location, aberrations, and efficiency. (A brief description of the ray tracing procedure is in the Appendix to this report.) In each case, the system performance was compared with the desired performance and the analysis was repeated with parameter modifications. The design effort concluded with a selection of the system that best satisfied the design goals or appeared to show promise.

Initially we considered only a few design approaches, but later considered other systems for a total of nine. The approaches are listed in Table I; the names given to the approaches, and in fact the distinctions among the approaches,

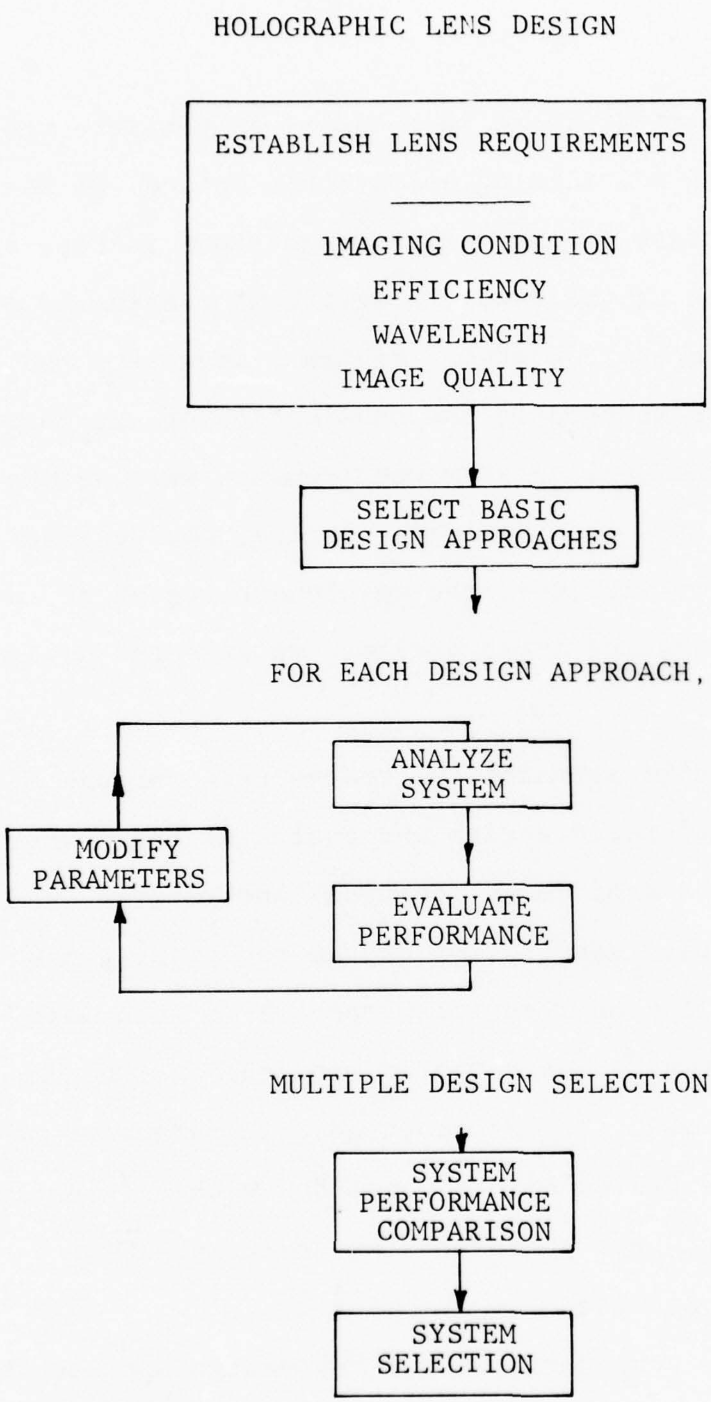

FIGURE 2. Procedure Used to Design and Analyze the Holographic Goggle.

TABLE I. DESIGN APPROACHES

ALL-HOLOGRAPHIC SYSTEMS	
PRELIMINARY DESIGN	SYSTEM 1
VIRTUAL IMAGE DESIGN	SYSTEM 2
TILTED ELEMENT DESIGN	SYSTEM 6
F-O TWIST DESIGN	SYSTEM 8
HYBRID SYSTEMS	
NEGATIVE EYELENS DESIGN	SYSTEM 3
INTER-ELEMENT LENS DESIGN	SYSTEM 4
TILTED ELEMENT HYBRID DESIGN	SYSTEM 5
POSITIVE EYELENS DESIGN	SYSTEM 7
TWO LENS DESIGN	SYSTEM 9

SEVEN DESIGNS PROVIDE FOR IMAGE INVERSION, SYSTEMS 2 AND 8 DO NOT.

are arbitrary, but serve to organize the various modifications to the basic system. The approaches in Table I are divided into two categories, those with all-holographic optics and those with combinations of holographic and conventional optics, or hybrid systems. Of the nine designs, seven provide for image inversion while two do not.

In the following pages we summarize each design approach with a brief discussion, sketches of the system and recording configurations, and a table of system characteristics. Many of the designs had such poor performance after a limited amount of analysis that further design modifications were not considered. Those designs that responded well to parameter modifications were pursued in greater detail to better gauge their ultimate potential. In most designs, one or both hologram diameters are larger than necessary, or optimum, as we were concerned more with ray directions and efficiencies than with packaging considerations.

The holograms in every case are assumed to be of the reflection type in which the two recording wavefronts are incident from the opposite sides of the hologram substrate. Except where noted, we assume a hologram thickness of 15 μm and a refractive index modulation of 0.03. The sketches show the recording geometry, approximately to scale, usually with one wavefront divergent and the other convergent. The relative position and orientation of the system element are shown in the reconstruction sketches, but the ray directions are approximate and serve to indicate in a qualitative manner imaging by the system.

We took two approaches to analyzing the performance of the various designs: in five we assumed points on the phosphor screen as input and determined where and how well the system formed an image of the screen, and in the remaining four we began with parallel light incident on the exit pupil and traced rays backwards through the system for various field angles to determine the image location (ideally on the phosphor screen).

Finally, since the basic system is symmetric about the axis passing through the image itensifier, we analyzed only one side of the system. For the complete system, the hologram designs are unchanged. To realize the design, the first hologram would probably be exposed to the two recording wavefronts, rotated 180° about its surface normal, and exposed again.

3.1 PRELIMINARY DESIGN

This is the first in a series of designs in which rays are traced from the phosphor screen to some location where an image of the screen is formed. It is assumed that in a system of this sort a conventional lens would be used between the image and the eye in a manner similar to the eyepieces of the current two-tube goggle. The objective of the holographic lenses, therefore, is to split the light from the phosphor screen and form for each eye an inverted image of the screen that in turn can be properly imaged at infinity by an eyepiece. (Since the primary interest is in the image formed by the holographic portion of the optical system, we restricted many of our investigations to the study of this intermediate image.)

For the Preliminary Design approach, two hologram lenses are used to form a real image of the phosphor screen between the eye and the secondary hologram lens, as shown in Figure 3. The hologram lenses invert the image so that the fiber-optic twist is not necessary. Figure 4 shows the construction parameters for each hologram lens (parameter definitions and sign conventions are given in the appendix).

The system performance characteristics are summarized in Table II. We were interested in determing the image positions of points at the center and ends of the phosphor screen. Given that the screen has a diameter of 18 mm, we looked at the images formed of points at $x = 0, \pm 9$ mm on the screen. For most of these investigations we chose the separation between the phosphor screen and the first hologram lens to be 18 mm. This separation should be small to keep the system efficiency high, but must be large enough to permit the light diffracted by the first hologram lens to reach

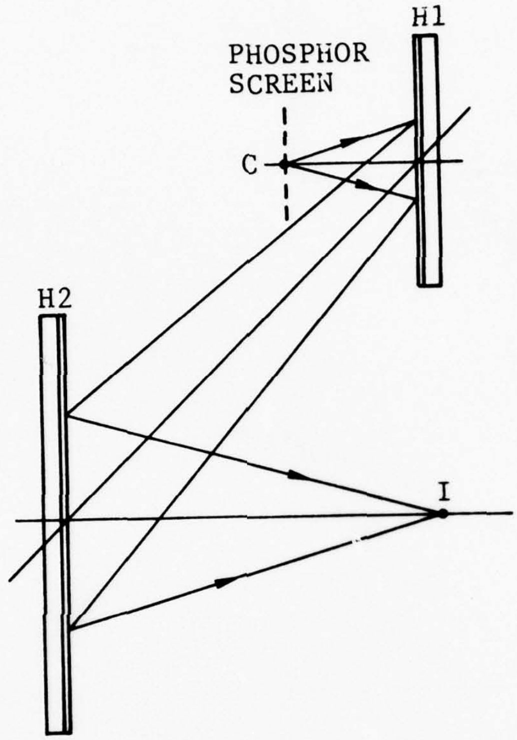

REC $x = 0$, $z = 18$ mm, D

SEPARATION $\alpha_{12} = -45^{\circ}$

$R_{12} = 72$ mm

FIGURE 3. PRELIMINARY DESIGN

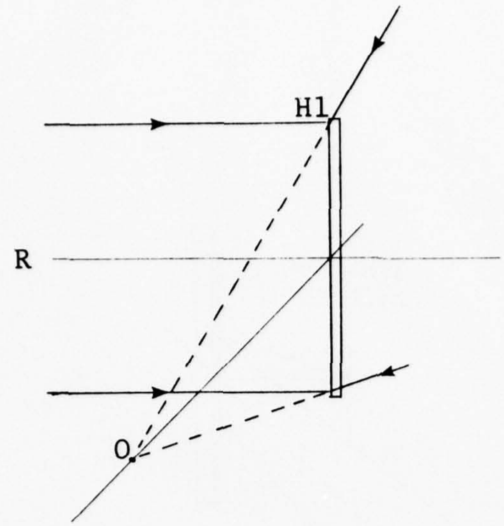

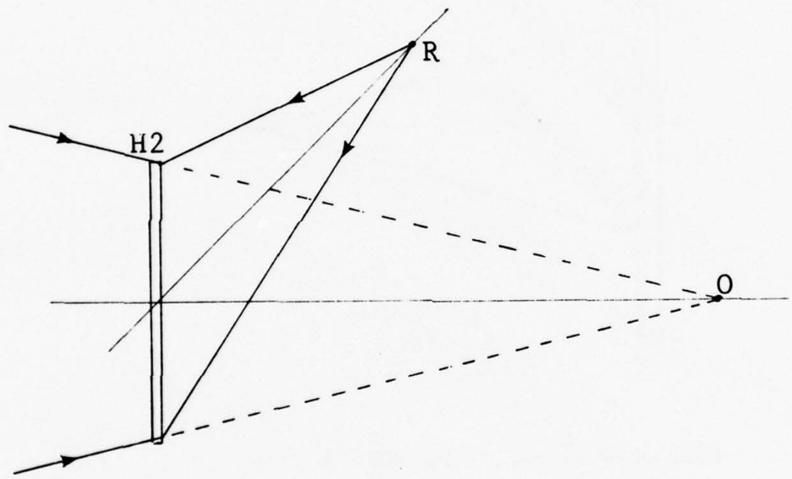

	HOL 1		HOL 2
REF	$\alpha = 0^{o}$, P	REF	$\alpha = -45^{o}$, R = -52 mm, D
OBJ	$\alpha = -45^{o}$, R = 40 mm, C	OBJ	$\alpha = 0^{o}$, R = -80 mm, D
DIA	36 mm	DIA	60 mm

FIGURE 4. CONSTRUCTION DETAILS OF PRELIMINARY DESIGN

TABLE II: SYSTEM 1

PRELIMINARY DESIGN

RECONSTRUCTION POINT X_c	IMAGE LOCATION X_I	Z_I	ABERRATIONS	EFFICIENCY
9mm	-3.8mm	-50.2mm	1187 λ	65.6%
0	- .06	-53.5	1871	74.4
-9	5.8	-50.9	608	78.8

DESIGN CHARACTERISTICS

ALL-HOLOGRAPHIC SYSTEM

INVERTS IMAGE

CURVED IMAGE PLANE

IMAGE DISTORTED

EFFICIENT

MAJOR LIMITATION

LARGE ABERRATIONS

unobstructed the secondary hologram lens.

The major limitation of this design is the large amount of aberrations. The aberrations listed in Table II represent the maximum deviation of the actual wavefront from the reference sphere centered at the gaussian image point. Because the aberrations are so large we do not show the individual terms, but state that coma and astigmatism were dominant.

3.2 VIRTUAL IMAGE DESIGN

This design approach is similar to the previous approach except that the image of the phosphor screen is an erect virtual image formed to the left of the secondary hologram lens. The system is shown in Figure 5 and the construction details are shown in Figure 6. Table III summarizes the performance characteristics of the system. Again, the aberrations are quite large (astigmatism dominant), and here the imaging is quite poor. At $x_c = -9$ mm, for example, the image is formed well to the right of the secondary hologram lens.

3.3 NEGATIVE EYELENS DESIGN

This system is similar to the Preliminary Design described in Section 3.1 but a negative lens has been added as shown in Figure 7. Although the lens moves the image of the phosphor screen to the right (towards the eye) it does not significantly affect the design characteristics obtained previously. Thus the aberrations continue to be unacceptably large and the

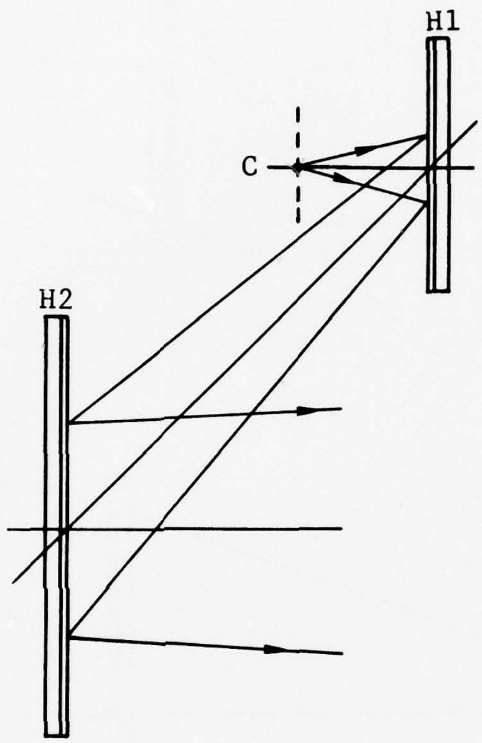

REC $x = 0$, $z = 18$ mm, D
SEPARATION $\alpha_{12} = -45^{\circ}$
$R_{12} = 72$ mm

FIGURE 5. VIRTUAL IMAGE DESIGN

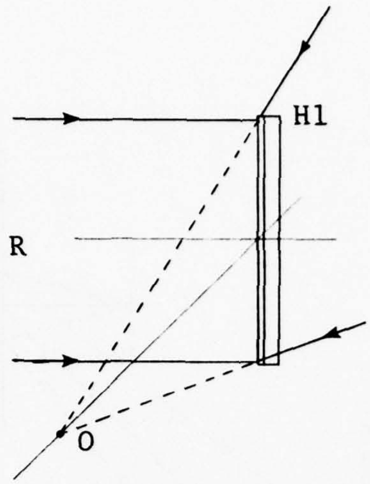

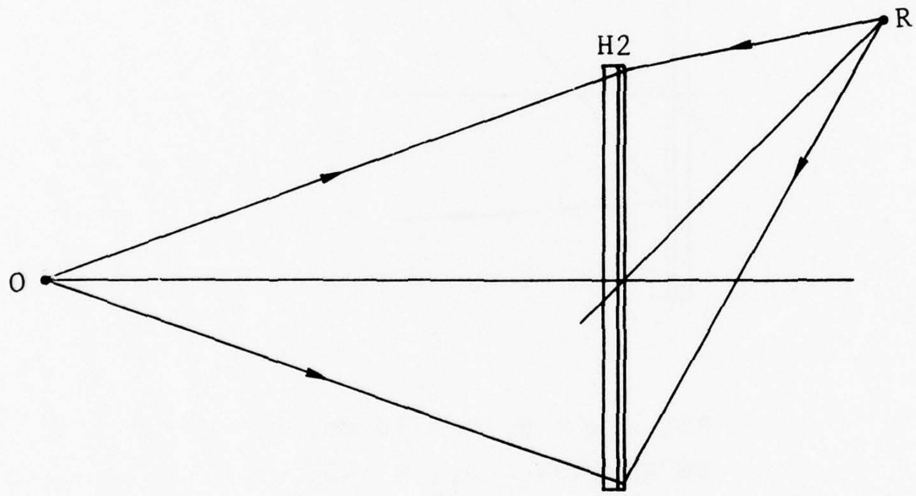

	HOL 1		HOL 2
REF	$\alpha = 0^{\circ}$, P	REF	$\alpha = -45^{\circ}$, R = -52 mm, D
OBJ	$\alpha = -45^{\circ}$, R = 35 mm, C	OBJ	$\alpha = 0^{\circ}$, R = 80 mm, C
DIA	36 mm	DIA	60 mm

FIGURE 6. CONSTRUCTION DETAILS OF VIRTUAL IMAGE DESIGN

TABLE III: SYSTEM 2

VIRTUAL IMAGE DESIGN

RECONSTRUCTION POINT X_c	IMAGE LOCATION X_I	Z_I	ABERRATIONS	EFFICIENCY
9mm	17.4mm	194mm	1330λ	68.4%
0	.13	261	2671	75.3
-9	1060	-5854	682	79.8

DESIGN CHARACTERISTICS

ALL-HOLOGRAPHIC SYSTEM

DOES NOT FORM LOCALIZED IMAGE

LARGE ABERRATIONS

MAJOR LIMITATION

POOR IMAGING

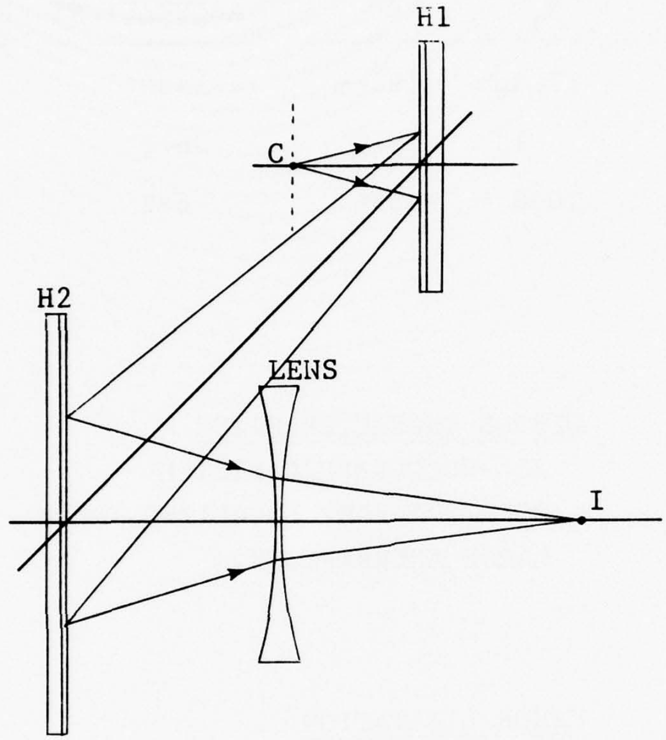

REC $x = 0$, $z = 18$ mm, D

SEPARATION $\alpha_{12} = -45^{\circ}$ $\alpha_{23} = 0^{\circ}$

$R_{12} = 72$ mm $R_{23} = -30$ mm

FIGURE 7. NEGATIVE EYELENS DESIGN

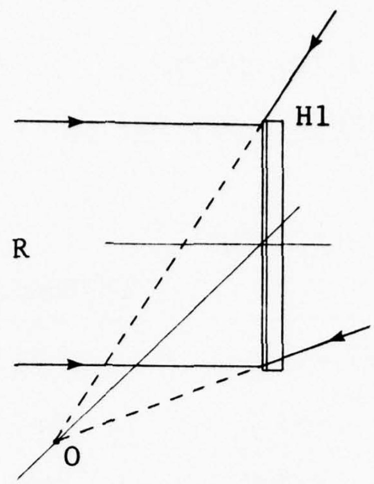

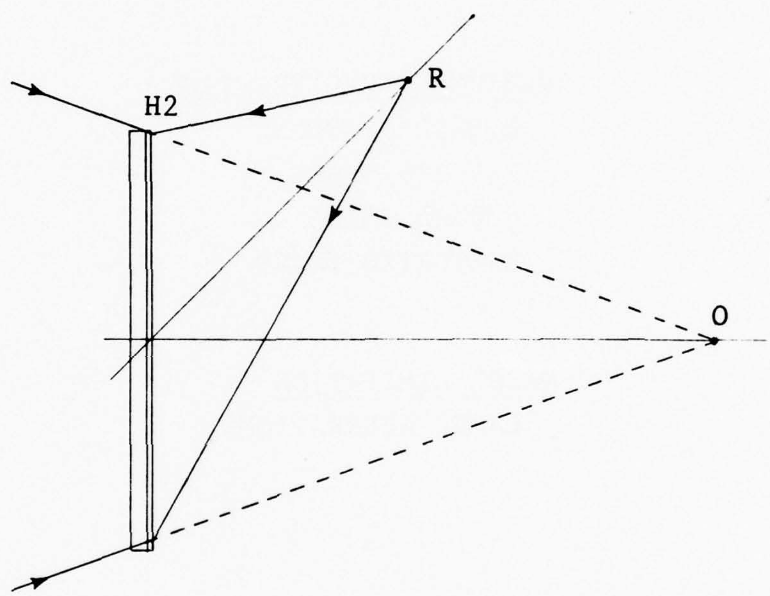

	HOL 1		HOL 2
REF	$\alpha = 0^{o}$, P	REF	$\alpha = -45^{o}$, R = -52 mm, D
OBJ	$\alpha = -45^{o}$, R = 35 mm, C	OBJ	$\alpha = 0^{o}$, R =-80 mm, C
DIA	36 mm	DIA	60 mm

FIGURE 8. CONSTRUCTION DETAILS OF NEGATIVE EYELENS DESIGN

TABLE IV: SYSTEM 3

NEGATIVE EYELENS DESIGN

RECONSTRUCTION POINT X_c	IMAGE LOCATION X_I	Z_I	ABERRATIONS	EFFICIENCY
9mm	-5.7mm	-30.6mm	1876λ	65.6%
0	- .12	-43.2	2367	74.4
-9	9.4	-36.8	570	74.8

DESIGN CHARACTERISTICS

HYBRID SYSTEM

INVERTS IMAGE

CURVED IMAGE

DISTORTED IMAGE

MAJOR LIMITATION

LARGE ABERRATIONS

image is curved and distorted. By image distortion we mean that for two object points located symmetrically about the optic axis, the corresponding two image points are not located symmetrically about the axis.

The efficiency of all the designs considered thus far is good, in excess of 70% on axis and reasonably uniform across the field. The efficiencies given throughout this report are holographic efficiencies: we assume no losses due to absorption or reflection at any surface. The holograms are assumed to be volume phase holograms that diffract light with high efficiency (100% theoretical potential) over a limited range of wavelengths and angles. Since the diffraction efficiency may be very low at other angles or wavelengths, the efficiency of the diffraction process is of greatest importance in the early considerations of system efficiency.

3.4 INTER-ELEMENT LENS DESIGN

Inversion of the image requires that the hologram lenses have relatively short focal lengths. Although there are two holograms over which to distribute the optical power, the requirements are nonetheless very demanding on the hologram performance. To alleviate the power requirements on the holograms, in this design we add a conventional lens element between the hologram lenses as shown in Figure 9.

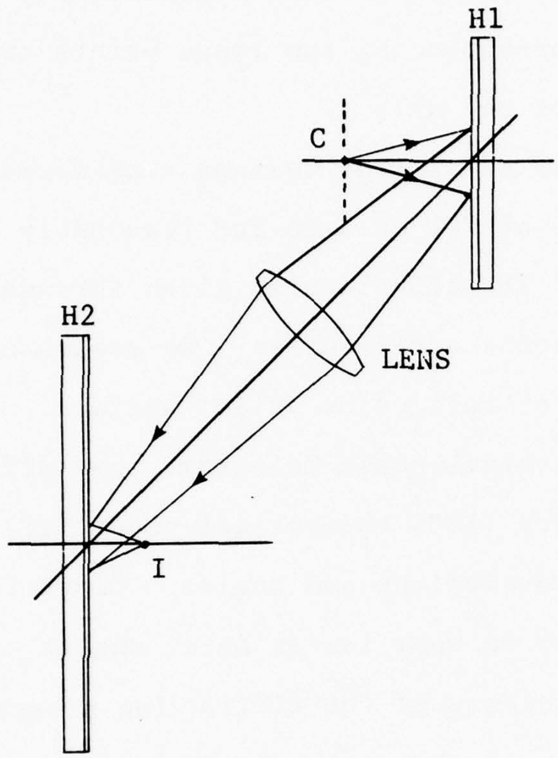

REC x = 0, z = 18 mm, D

SEPARATION $\alpha_{12} = -45^{\circ}$ $\alpha_{23} = 0^{\circ}$

$R_{12} = 30$ mm $R_{23} = 42$ mm

LENS

SURF 1 CV = 41.67 m^{-1}

SURF 2 CV = -41.67 m^{-1}

INDEX 1.5

DIA 20 mm

FIGURE 9. INTER-ELEMENT LENS DESIGN

Construction parameters are shown in Figure 10; note that the secondary hologram lens (H2) has a diameter considerably larger than would be necessary in an actual system. From the design characteristics of Table V we see that the system performance is quite poor. For object points $x_c \leq 0$ the imaging is somewhat improved over earlier designs but the efficiency falls off rapidly, whereas for $x_c > 0$, the imaging becomes very poor.

3.5 TILTED ELEMENT HYBRID DESIGN

A considerable improvement in performance is realized by reducing the power of the inter-element lens and tilting the secondary hologram, H2, as shown in Figure 11. The recording parameters of the holographic elements are given in Figure 12. From the design characteristics given in Table VI, we see that this design shows somewhat improved imaging with good efficiency. Although the aberrations are still large, they have been reduced considerably. The image distortion has been reduced from some of the previous designs, but the image plane is tilted to a considerable degree.

3.6 TILTED ELEMENT DESIGN

In this and the remaining designs, the system is analyzed by tracing rays backwards through the optical system from the exit pupil to the phosphor screen. We are interested

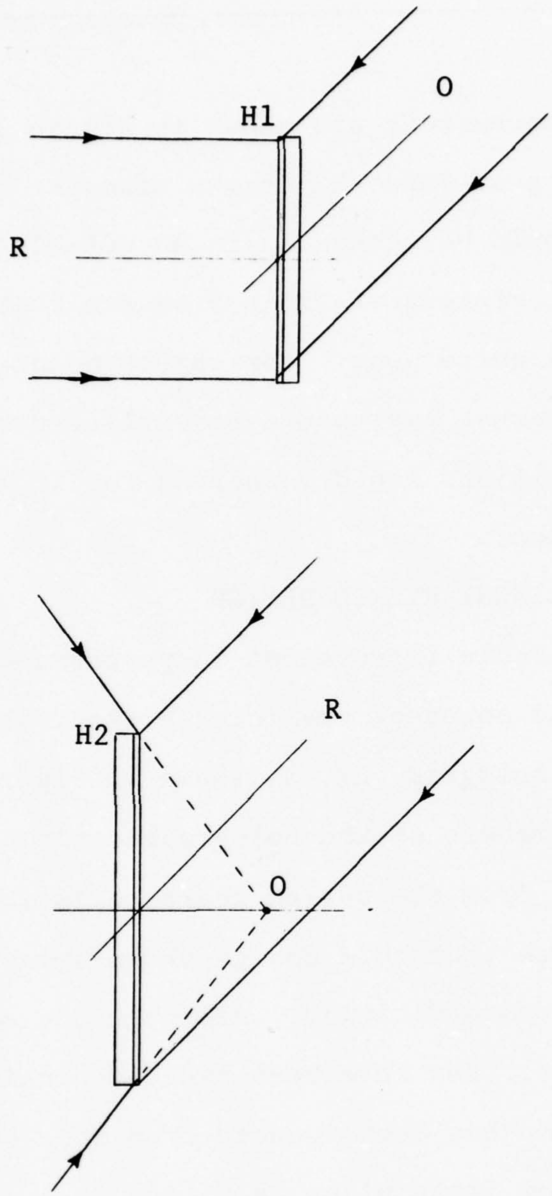

	HOL 1		HOL 2
REF	α = 0, P	REF	$\alpha = -45^{o}$, M
OBJ	$\alpha = -45^{o}$, M	OBJ	$\alpha = 0^{o}$, R = -18 mm, C
DIA	36 mm	DIA	60 mm

FIGURE 10. CONSTRUCTION DETAILS OF INTER-ELEMENT LENS DESIGN

TABLE V: SYSTEM 4

INTER-ELEMENT LENS DESIGN

RECONSTRUCTION POINT X_c	IMAGE LOCATION X_I	Z_I	ABERRATIONS	EFFICIENCY
9mm	-25.6mm	33.2mm	3024λ	35.4%
0	- .006	-8.29	189	73.2
-9	5.6	-8.71	209	1.03

DESIGN CHARACTERISTICS

HYBRID SYSTEM

INVERTS IMAGE

VERY POOR PERFORMANCE

MAJOR LIMITATION

POOR IMAGING

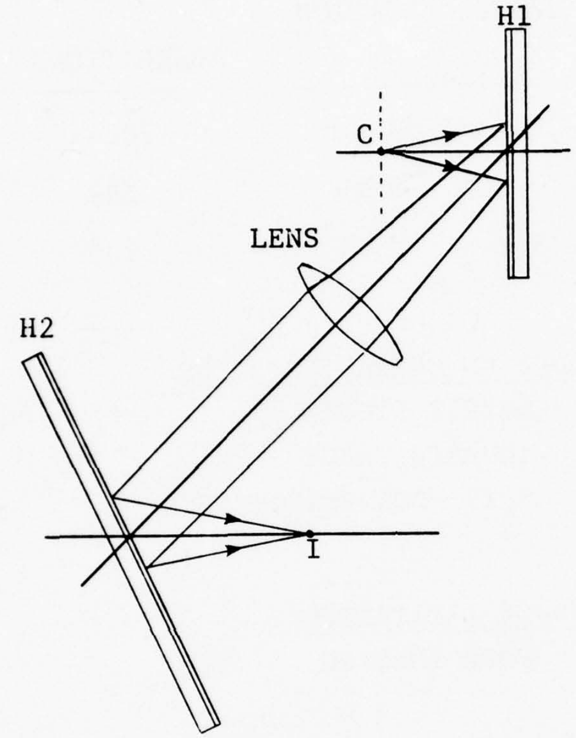

REC $x = 0$, $z = 18$ mm, D

SEPARATION $\alpha_{12} = -45^\circ$ $\alpha_{23} = 0^\circ$

$R_{12} = 30$ mm $R_{23} = 42$ mm

EULER ROTATION H2 $\beta = -20^\circ$

LENS

SURF 1 CV = 24 m^{-1}

SURF 2 CV = -24 m^{-1}

INDEX 1.5

DIA 20 mm

FIGURE 11. TILTED ELEMENT HYBRID DESIGN

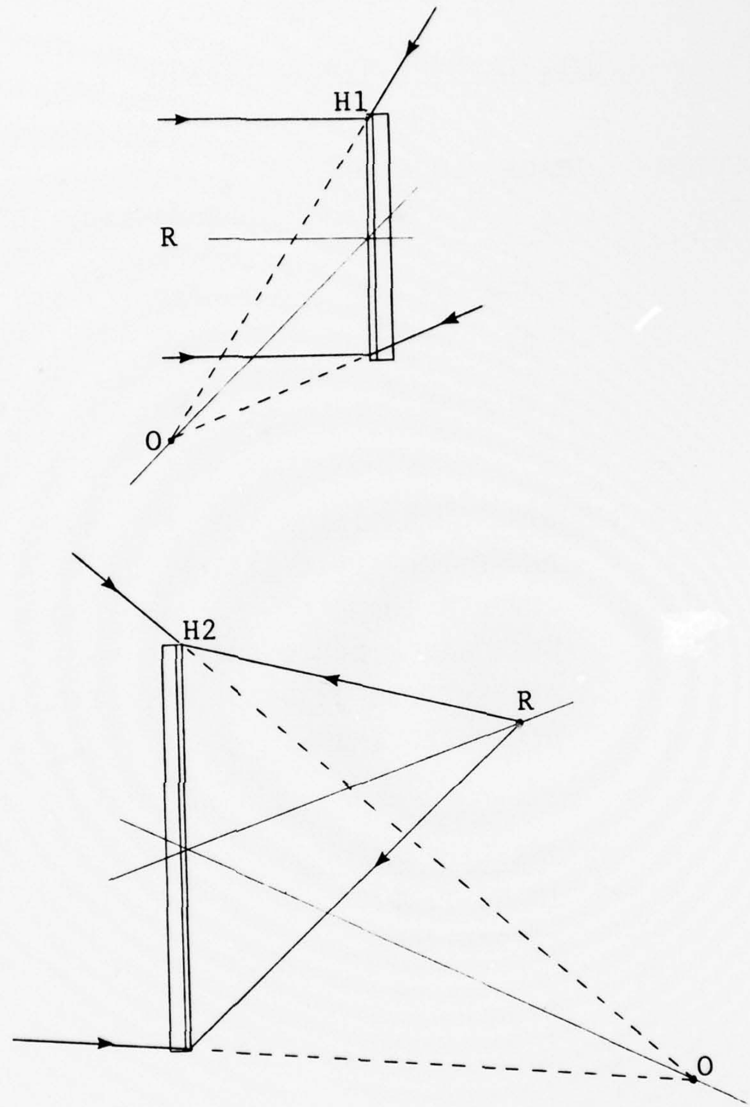

HOL 1		HOL 2	
REF	$\alpha = 0^{o}$, P	REF	$\alpha = -20^{o}$, R = -52 mm, D
OBJ	$\alpha = -45^{o}$, R = 40 mm, C	OBJ	$\alpha = 25^{o}$, R = -80 mm, C
DIA	36 mm	DIA	60 mm

FIGURE 12. CONSTRUCTION DETAILS OF TILTED ELEMENT HYBRID DESIGN

TABLE VI: SYSTEM 5

TILTED ELEMENT HYBRID DESIGN

RECONSTRUCTION POINT X_c	IMAGE LOCATION X_I	Z_I	ABERRATIONS	EFFICIENCY
9mm	-5.3mm	11.2mm	336λ	64.6%
0	- .03	13.8	165	71.3
-9	7.2	19.2	89	69.3

DESIGN CHARACTERISTICS

ALL-HOLOGRAPHIC SYSTEM

INVERTS IMAGE

REASONABLE EFFICIENCY

ABERRATIONS REDUCED, BUT STILL LARGE

DISTORTED IMAGE

MAJOR LIMITATIONS

IMAGE TILT

ABERRATIONS

in determining the point focus at the phosphor screen over the $\pm 20^{o}$ range of field angles (at the exit pupil). This design is similar to the previous system, but the inter-element conventional lens has been removed. Figure 13 shows the system in reconstruction and Figure 14 shows the construction geometry of the hologram elements.

The performance of the system is rather poor as indicated by the data in Table VII. In addition to a fall-off in efficiency at field angles other than zero, the aberrations are quite large, with approximately the same amount of spherical, coma, and astigmatism at $\alpha_c = 0$ but with astigmatism dominant at $\alpha_c = \pm 20^{o}$. The image has a great deal of distortion and lies on a tilted plane.

3.7 POSITIVE EYELENS DESIGN

In this design a conventional lens with positive power is placed between the secondary hologram lens and the exit pupil (15 mm from the exit pupil) as shown in Figure 15. Construction geometry of the hologram lenses is shown in Figure 16. From Table VIII we see that the system is characterized by large aberrations and image distortion. There is some image tilt and field curvature, but the latter could be accomodated by adding a fiber-optics plate to the phosphor screen, with the necessary curvature added to the free surface of the plate. Although there is a decrease in

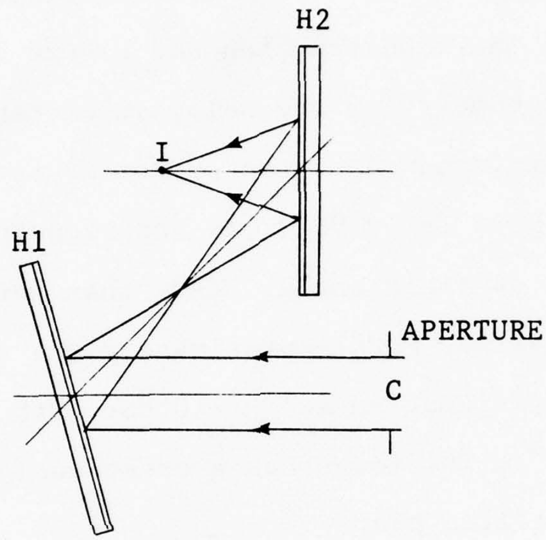

REC $\alpha = 0^{o}$, M

SEPARATION $\alpha_{12} = -30^{o}$

$R_{12} = -45$ mm

EULER ROTATION H1 $\beta = 15^{o}$

APERTURE DIA 10 mm

FIGURE 13. TILTED ELEMENT DESIGN

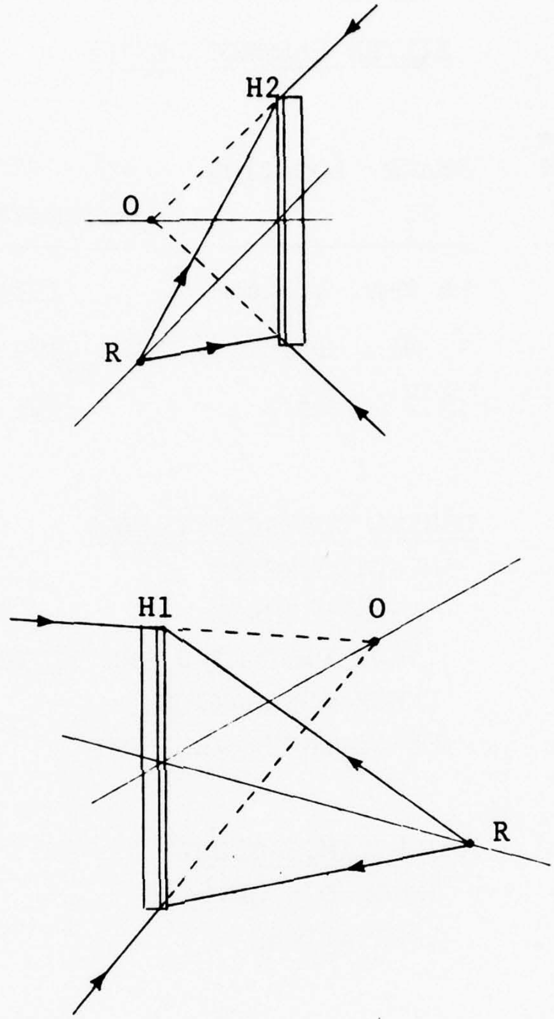

HOL 1		HOL 2	
REF	$\alpha = 15^{o}$, R = -45 mm, D	REF	$\alpha = -45^{o}$, R = 27.3 mm, D
OBJ	$\alpha = -30^{o}$, R = -35 mm, C	OBJ	$\alpha = 0^{o}$, R = 18 mm, C
DIA	40 mm	DIA	40 mm

FIGURE 14. CONSTRUCTION DETAILS OF TILTED ELEMENT DESIGN

TABLE VII: SYSTEM 6

TILTED ELEMENT DESIGN

RECONSTRUCTION ANGLE α_c	IMAGE LOCATION X_I	Z_I	ABERRATIONS	EFFICIENCY
20^o	-6.8mm	30.2mm	251λ	38.2%
0	- .01	18.5	399	82.6
-20	2.2	15.9	941	49.3

DESIGN CHARACTERISITCS

HYBRID SYSTEM

INVERTS IMAGE

IMAGE DISTORTED AND TILTED

LARGE ABERRATIONS

EFFICIENCY FALLS OFF

MAJOR LIMITATIONS

IMAGE DISTORTION

ABERRATIONS

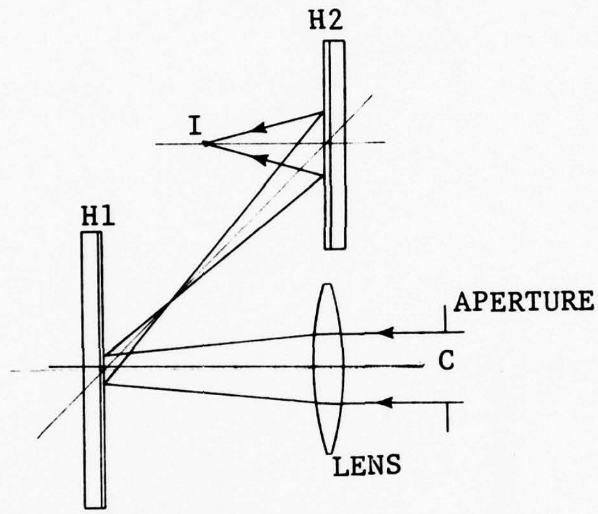

REC $\alpha = 0^o$, M

SEPARATION $\alpha_{12} = 0^o$ $\alpha_{23} = -45^o$

$R_{01} = 15$ mm $R_{23} = -45$ mm

$R_{12} = 30$ mm

APERTURE DIA 10 mm

LENS

SURF 1 CV = 14.3 m^{-1}

SURF 2 CV = -14.3 m^{-1}

INDEX 1.5

DIA 25 mm

FIGURE 15. POSITIVE EYELENS DESIGN

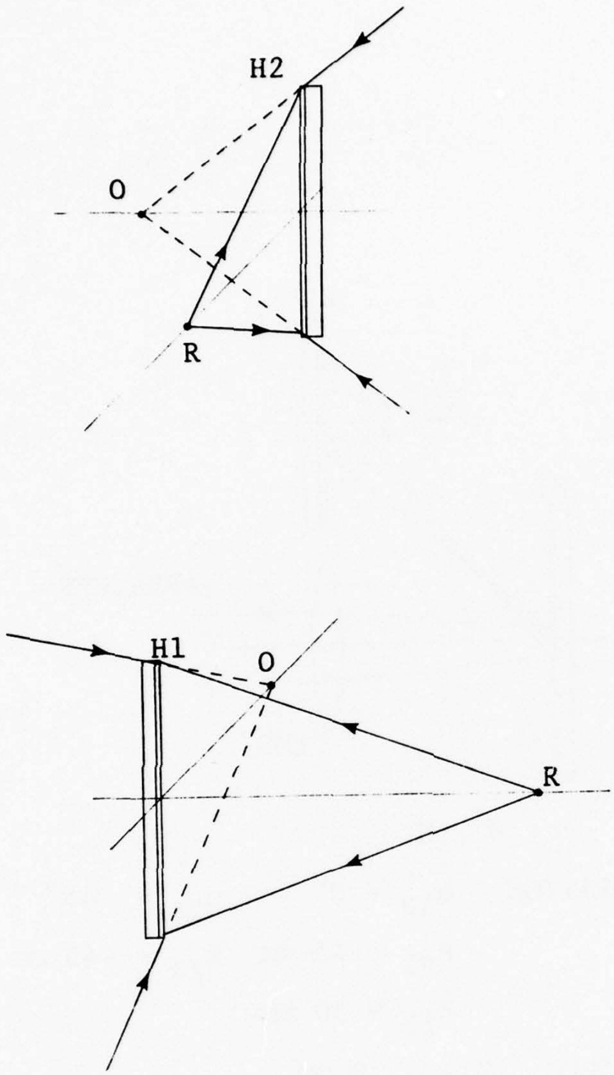

HOL 1		HOL 2	
REF	$\alpha = 0^{o}$, R = -53.5 mm, D	REF	$\alpha = -45^{o}$, R = 22.9 mm, D
OBJ	$\alpha = -45^{o}$, R = -22 mm, C	OBJ	$\alpha = 0^{o}$, R = 22.1 mm, C
DIA	40 mm	DIA	36 mm

FIGURE 16. CONSTRUCTION DETAILS OF POSITIVE EYELENS DESIGN

TABLE VIII: SYSTEM 7

POSITIVE EYELENS DESIGN

RECONSTRUCTION ANGLE α_c	IMAGE LOCATION X_I	Z_I	ABERRATIONS	EFFICIENCY
20^o	-5.0mm	14.6mm	107λ	78.0%
0	.01	17.1	1446	73.3
-20	2.7	16.4	893	35.0

DESIGN CHARACTERISTICS

HYBRID SYSTEM

INVERTS IMAGE

CURVED IMAGE

MAJOR LIMITATIONS

ABERRATIONS

IMAGE DISTORTION

efficiency for negative field angles, in the complete two-eye system, the decrease in efficiency at each eye would occur for opposite field angles, so that there might not be an apparent loss in image brightness across the field-of-view.

3.8 FIBER-OPTIC TWIST DESIGN

This system alone assumes that the image inversion is performed by a fiber-optic twist immediately following the phosphor screen. Relieved of the burden of inverting the image, the hologram lenses can have longer focal lengths than in previous designs, and thus should form images with higher quality. Figure 17 shows the system in reconstruction, with no image inversion. The relatively long construction beams of the holograms are evident in Figure 18. The system performance is characterized by low aberrations and a limited field-of-view that results from low diffraction efficiencies at field angles of more than a few degrees.

It may be possible to achieve high diffraction efficiency throughout the field-of-view by replacing the spherical object-beam wavefront of hologram H2 by a wavefront with a specially constructed phase surface. This would be done in such a way that the reconstructing rays at all field angles would fall within the region of Bragg diffraction. Such a wavefront falls in the category of arbitrary phase wavefronts and might be obtained through the use of aspheric optics

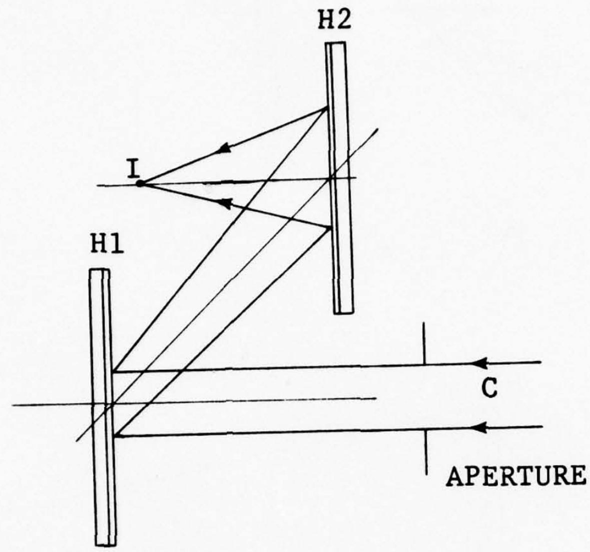

REC $\alpha = 0^o$, M

SEPARATION $R_{01} = 45$ mm

$\alpha_{12} = -45^o$

$R_{12} = -45$ mm

APERTURE DIA 10 mm

FIGURE 17. FIBER-OPTIC TWIST DESIGN

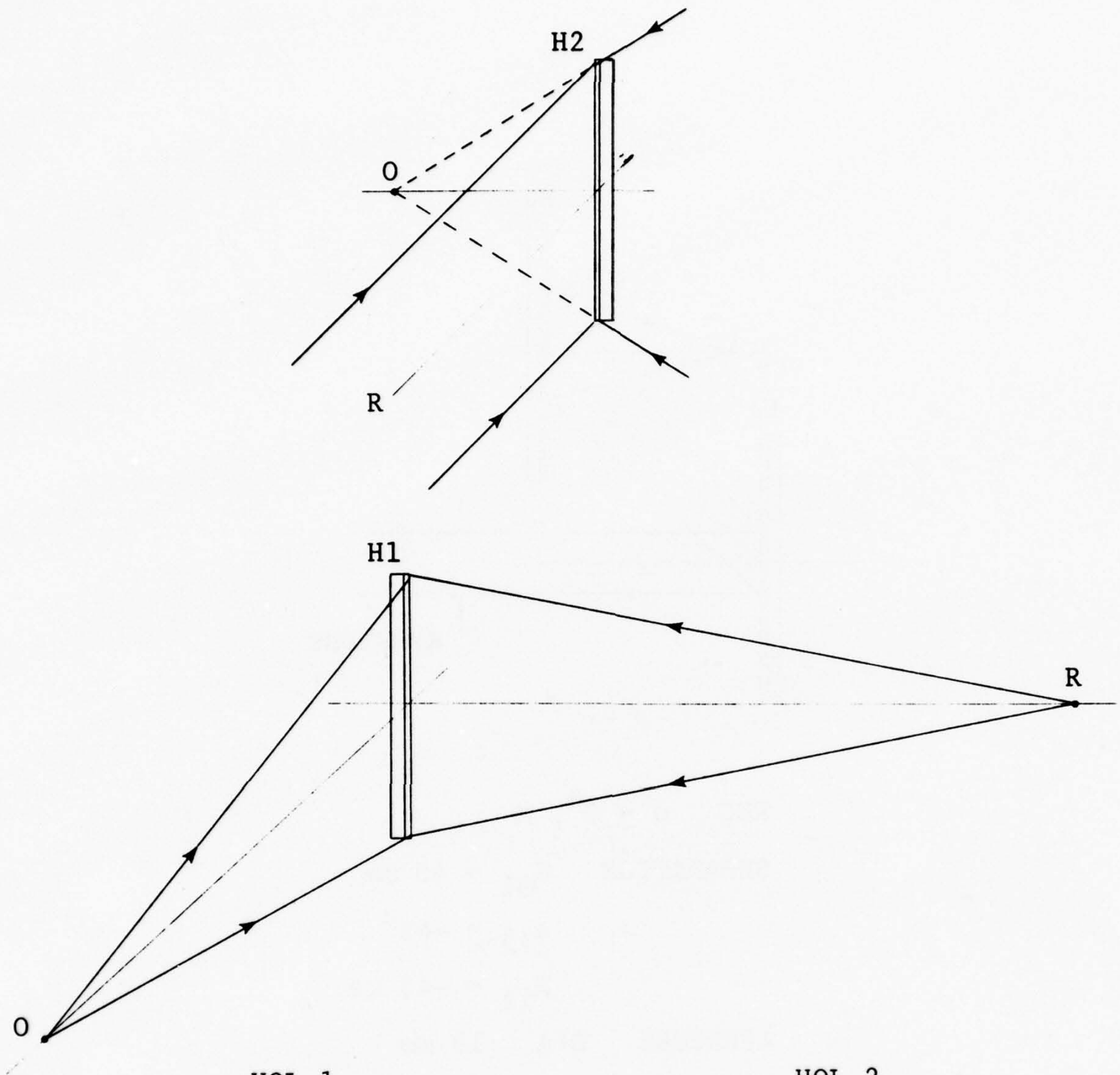

HOL 1		HOL 2	
REF	$\alpha = 0^{o}$, R = -100 mm, D	REF	$\alpha = -45^{o}$, P
OBJ	$\alpha = -42^{o}$, R = 75 mm, D	OBJ	$\alpha = 0^{o}$, R = 30 mm, C
DIA	30 mm	DIA	40 mm

FIGURE 18. CONSTRUCTION DETAILS OF FIBER-OPTIC TWIST DESIGN

TABLE IX: SYSTEM 8

FIBER-OPTIC TWIST DESIGN

RECONSTRUCTION ANGLE α_c	IMAGE LOCATION X_I	Z_I	ABERRATIONS	EFFICIENCY
10^o	7.9mm	24.7mm	0.048λ	2.33%
0	-1.3	27.5	8.9	94.8
-10	-5.6	37.9	0.59	0.71

THIRD ORDER ABERRATIONS

RECONSTRUCTION ANGLE	SPHERICAL	COMA	ASTIGMATISM
10^o	$8.9\times10^{-4}\lambda$	$.079\lambda$	$6.5\times10^{-5}\lambda$
0	27.0	64.4	12.0
-10^o	.028	2.4	4.1×10^{-4}

DESIGN CHARACTERISTICS

ALL-HOLOGRAPHIC SYSTEM

LOW ABERRATIONS

TILTED IMAGE PLANE

DOES NOT INVERT IMAGE

MAJOR LIMITATION

SMALL FIELD-OF-VIEW

BECAUSE OF EFFICIENCY FALL-OFF

or perhaps computer generated holograms.

3.9 TWO LENS DESIGN

This design adds two conventional lenses to the holographic elements as shown in Figure 19. In addition we have introduced curvature to the hologram lenses. The construction geometry of the two holograms is shown in Figure 20. The overall performance of this system is best of all the design approaches. Aberrations are approaching acceptable levels for visual systems and the efficiency is reasonably uniform over the 40^o field-of-view (for this design, we assumed a hologram thickness of $6\mu m$ and a refractive index modulation of 0.075). The image tilt of previous systems has been considerably reduced, but the image is still distorted.

We briefly examined the effect of changing the wavelength by up to $\pm 10nm$ for this design. The primary effect of changing the wavelength is lateral motion of the image due to lateral dispersion. For small field angles the image point (at the phosphor screen) moves a few tenths of a millimeter and the aberrations increase by approximately 50%. For field angles near $\pm 20^o$, the dispersion is somewhat greater, nearing three quarters of a millimeter. In addition, the aberrations become larger (on the order of 100 to 200 λ) with coma dominant for $\alpha_c = 20^o$ and comparable amounts of spherical, coma, and astigmatism for $\alpha_c = -20^o$.

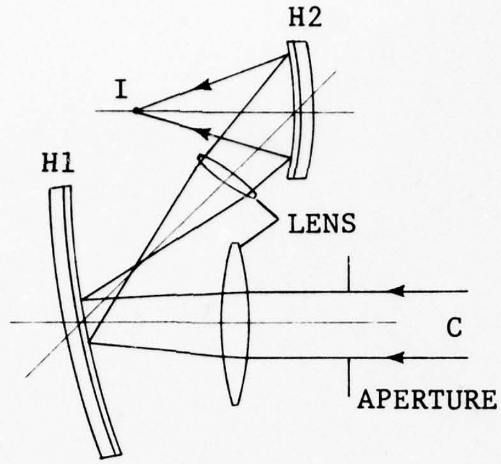

REC $\alpha = 0^{o}$, M

SEPARATION $\alpha_{01} = 0^{o}$, $R_{01} = 15$ mm

$\alpha_{12} = 0^{o}$, $R_{12} = 20$ mm

$\alpha_{23} = -45^{o}$, $R_{23} = -30$ mm

$\alpha_{34} = 0^{o}$, $R_{34} = -12$ mm

HOL 1 TILT 10^{o}

LENS 2 TILT 10^{o}

LENS 1		
	SURF 1	CV = 14.3 m^{-1}
	SURF 2	CV = -14.3 m^{-1}
	INDEX	1.5
	DIA	25 mm
LENS 2		
	SURF 1	CV = +25 m^{-1}
	SURF 2	CV = -25 m^{-1}
	INDEX	1.5
	DIA	10 mm

FIGURE 19. TWO LENS DESIGN

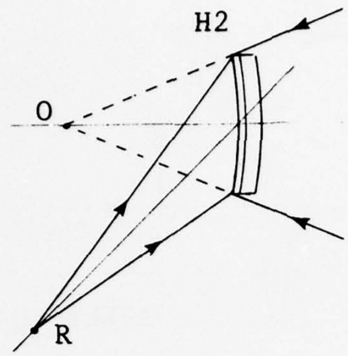

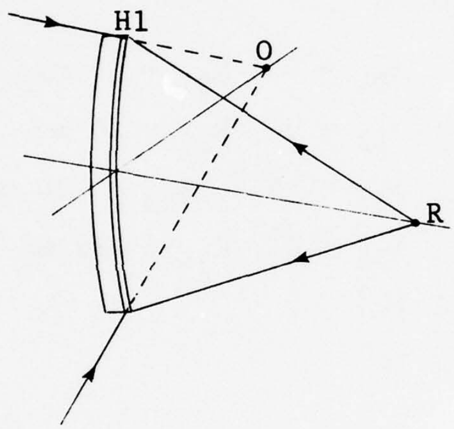

HOL 1	HOL 2
REF $\alpha = 10^{\circ}$, R = -43.5 mm, D	REF $\alpha = -45^{\circ}$, R = 40 mm, D
OBJ $\alpha = -35^{\circ}$, R = -26 mm, C	OBJ $\alpha = 0^{\circ}$, R = 25 mm, C
DIA 40 mm	DIA 36 mm
SURFACE CV -18 m^{-1}	SURFACE CV = 23 m^{-1}

FIGURE 20. CONSTRUCTION DETAILS OF TWO LENS DESIGN

TABLE X: SYSTEM 9

TWO LENS DESIGN

RECONSTRUCTION ANGLE α_c	IMAGE LOCATION X_I	Z_I	ABERRATIONS	EFFICIENCY
20^o	-4.1mm	23.6mm	34λ	67.9%
0	0.15	22.6	20	75.8
-20^o	8.2	21.9	81	52.4

THIRD ORDER ABERRATIONS

RECONSTRUCTION ANGLE	SPHERICAL	COMA	ASTIGMATISM
20^o	51.0λ	167λ	28.3λ
0	51.0	55.6	3.54
-20	37.8	158	45.7

DESIGN CHARACTERISTICS

HYBRID SYSTEM

MODERATE ABERRATIONS

INVERTS IMAGE

IMAGE TILT REDUCED

SHOWS PROMISE

MAJOR LIMITATION

IMAGE DISTORTION

Finally, since this design has shown the most promise, in Figure 21 we show a sketch of the system indicating the paths of two ray bundles, at $\alpha_c = 0^o$ and at $\alpha_c = +20^o$. Note that the interelement lens is closer to the primary hologram lens than optimum. We found that this lens position minimizes aberrations, but anticipate that a better position can be found (still with moderate aberrations) if we modify certain other system parameters as well as the lens location.

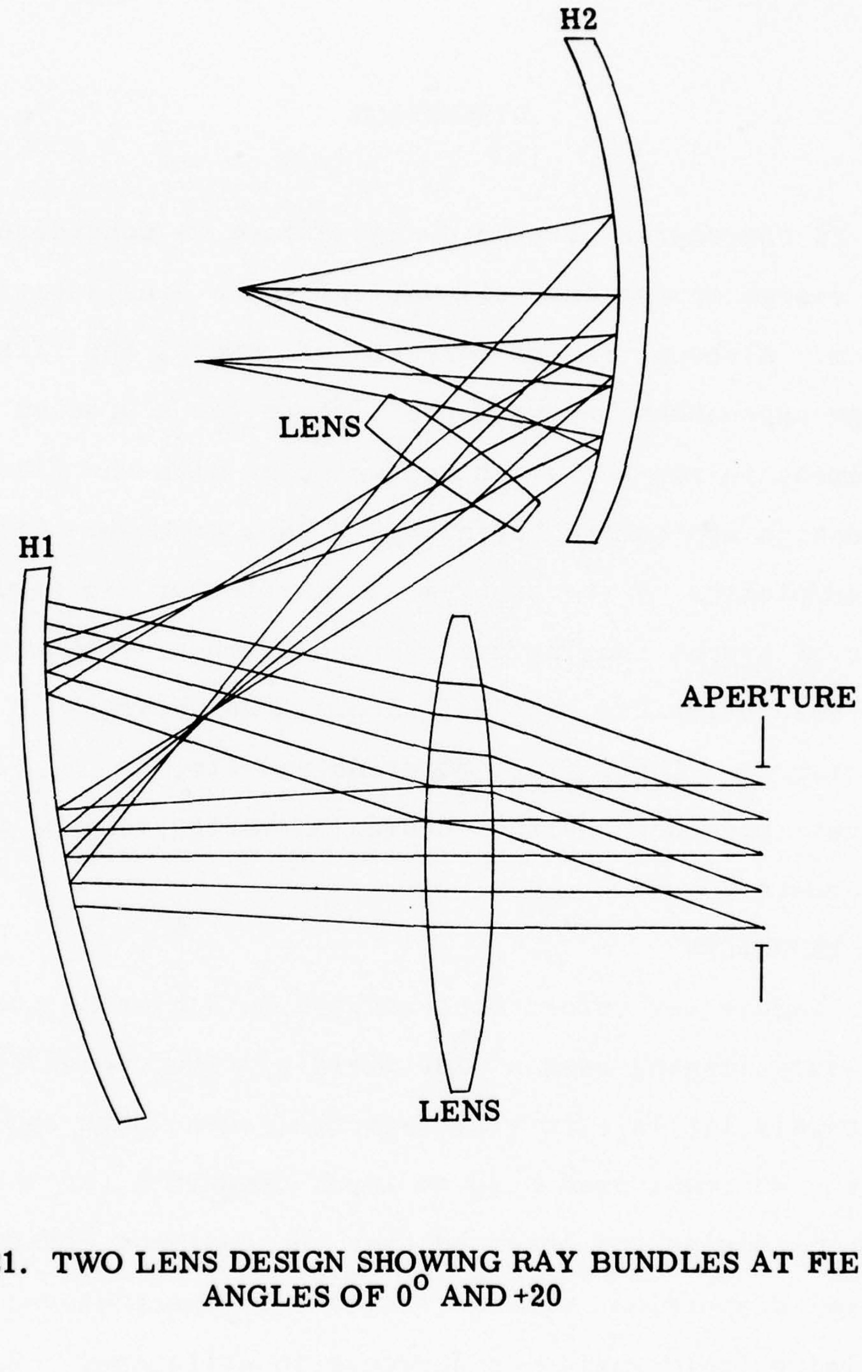

FIGURE 21. TWO LENS DESIGN SHOWING RAY BUNDLES AT FIELD ANGLES OF 0° AND +20

4
DISCUSSION

In the course of this design effort we considered nine design approaches, all variants of a single basic system. Although the performance of some of the first design approaches was very poor, there was a gradual improvement in the system characteristics with the final two design approaches beginning to show promise. Given the complexity of the problem, in particular the requirements of proper imaging over a wide field-of-view with good resolution and high efficiency, the progress is most encouraging. The limited duration and size of the effort, however, precluded further design investigations or improvements.

4.1 BANDWIDTH

Because our effort concentrated on achieving the necessary imaging over a wide field-of-view, we devoted relatively little effort to (spectral) bandwidth considerations. We considered a 20 nm input bandwidth for the Two Lens Design and observed that the dominant effect was lateral dispersion, with an increase in aberrations, and, for large field angles, a decrease in efficiency. We anticipate serious difficulties with an input comparable to that of the P-20 phosphor, where the bandwidth is over

100 nm. Achromatization techniques have been developed for holographic optics systems,[8-10] but since these work for specific configurations, they may not be applicable to the night glass system. A preferable solution is to substitute a phosphor with a narrower output spectrum such as the P-44 or P-45 phosphors. (In most holographic optical systems using phosphors, the phosphor is carefully selected to match systems requirements). The total energy output and costs of the different phosphors must be examined in considering such a substitution.

Volume phase reflection holograms of the type we have assumed are highly efficient over a bandwidth of approximately 20 nm; rays outside this spectral region are diffracted with very low efficiency. If the input is derived from a relatively broadband source such as the P-20 phosphor, the hologram lenses will diffract efficiently only a portion of the bandwidth. Although this tends to alleviate the chromatic problems associated with the hologram lenses, it is wasteful of light in a system that requires the efficient use of light.

There exists a technique which, in principle, should allow us to use volume reflection holograms efficiently over a broader spectral region than their normal bandwidth and at the same time achieve a limited amount of achromatization. With this technique we record on the same hologram medium, several hologram lenses, each of which is recorded with the necessary geometry to image efficiently and properly at different wavelength regions that are separated according to the bandwidth of each individual hologram. The holograms may have the same recording wavelength but slightly altered recording geometries (as determined with the aid of the ray-tracing design programs), or, alternatively, they may have the same geometry but different recording wavelengths. Recording several holograms in the same volume of the recording medium is very demanding on the material capabilities. Although we have achieved considerable success in other programs in forming efficient multiple-grating holograms,(11,12) it may be necessary to record holograms on separate substrates and later put them together in a stacked configuration.

4.2 ABERRATIONS

Throughout the previous section we indicated the magnitude of the aberrations for different field angles of the various design approaches. The aberrations were determined by first locating the Gaussian image, defining a reference sphere centered at the Gaussian image location, and determining the deviations of the actual wavefront from the reference sphere. Although we computed the

12. W.S. Colburn and B.J. Chang "Evaluation of Hologram Optical Elements", ARPA Quarterly Technical Report, Report No. 194500-5-T, Environmental Research Institute of Michigan, August 1974.

amounts of spherical, coma, and astigmatism that were present, for most of this investigation we were primarily interested in the maximum deviation of the wavefront from the reference sphere.

For a visual system it is not a simple matter to specify a certain amount of aberration as representing a good image and a greater amount as indicating a marginal image. Rather, one must consider the problem in greater detail, examining, for example, the relative magnitudes of the third order coefficients. In most of our design approaches, the aberrations were so large as to preclude the necessity of looking beyond the maximum wavefront deviation. In fact, we felt that to show promise, the maximum deviation from the reference sphere (in optical path difference, or OPD) should be less than about 40 λ. Although the last two design approaches had aberrations of this magnitude or less, the preliminary nature of our investigations did not permit detailed examination of the image quality of these systems, but only the observation that unlike the previous systems, these show sufficient promise to merit further investigation. Determination of the MTF of any of the systems also seemed premature for this phase of the effort.

In our analysis of the various designs, some rays were diffracted with very low efficiencies. Because of the present structure of the ray-tracing programs, these rays are not deleted from the rayset, and are thus included in the image and aberration calculations. These rays tend to be marginal rays of the system, and thus often contribute heavily to the aberrations, yet would contribute very little to the image of a real system because of their low intensities. For much of our analysis, the aberrations were so large that considerations of this sort were of little meaning. We have reached the point now, however, where further investigations might be more meaningful if an intensity threshold were established, below which rays would be deleted from the rayset. We would expect in most cases some reduction in the maximum wavefront deviations.

4.3 HYBRID AND ALL-HOLOGRAPHIC DESIGNS

In Table I we divided the systems into two groups according to whether they were all-holographic or included conventional as well as holographic optics. Although the optical system is more complex, hybrid systems offer the possibility of distributing the optical power over more elements, and provide additional variables for the designer to adjust to achieve the desired system characteristics. The conventional lens elements should be relatively simple to minimize the weight added to the goggle. In the

Two Lens Design, some additional complexity is introduced by tilting the interelement lens by 10° with respect to the optical axis joining the hologram centers.

The all-holographic systems offer the potential of relatively simple and lightweight optical systems. In these systems or in hybrid systems in which there is no lens between the exit pupil and the secondary hologram lens, we can take advantage of the wavelength and angular selectivity of the hologram lens. At angles and wavelengths that are not strongly diffracted by the hologram lens, the observer will be able to see through the lens to look, for example, at an instrument panel.

The eighth system analyzed, the Fiber-Optics Twist Design, is an all-holographic system characterized by relatively low aberrations but very low efficiencies at most field angles. It may prove possible to achieve reasonable efficiencies at all field angles by recording one or both holograms with a special wavefront which has a suitably tailored phase front.

4.4 ARBITRARY PHASE WAVEFRONTS

The hologram lenses we considered in this investigation, and indeed, nearly all hologram lenses, are recorded with two spherical wavefronts (often one wavefront is plane, a spherical wavefront of infinite radius). Since it is usually preferable to construct the hologram with a single exposure to the two wavefronts, the designer is limited in his ability to tailor the hologram to meet certain performance criteria. One method of increasing the designer's options is to allow construction wavefronts with arbitrary phase surfaces (rather than spherical phase surfaces). With such construction wavefronts, we could exercise far more control over the hologram parameters at every point on the hologram. If we could so properly adjust the fringe structure in the hologram lenses of the Fiber-Optics Twist Design, for example, we could achieve high efficiencies across the entire field-of-view.

For completeness, let us briefly consider how we might realize arbitrary phase wavefronts to construct hologram lenses. One method would be to introduce non-spherical conventional optics into the construction beam, as shown in Figure 22. The non-spherical optics might be aspherics, cylinders, toroids, or, indeed, have a surface of any shape other than spherical. Another approach, which appears very exciting at this time, is to introduce a computer generated hologram into the construction beam, as shown in Figure 23. The computer generated hologram might be of the in-line ROACH type[13] and would probably be generated for the specific requirements of a given hologram lens design.

---

13. D.C. Chu, J.R. Fienup, and J.W. Goodman, "Multiemulsion On-Axis Computer Generated Hologram", Appl. Opt. 12, pp. 1386-8, July 1973.

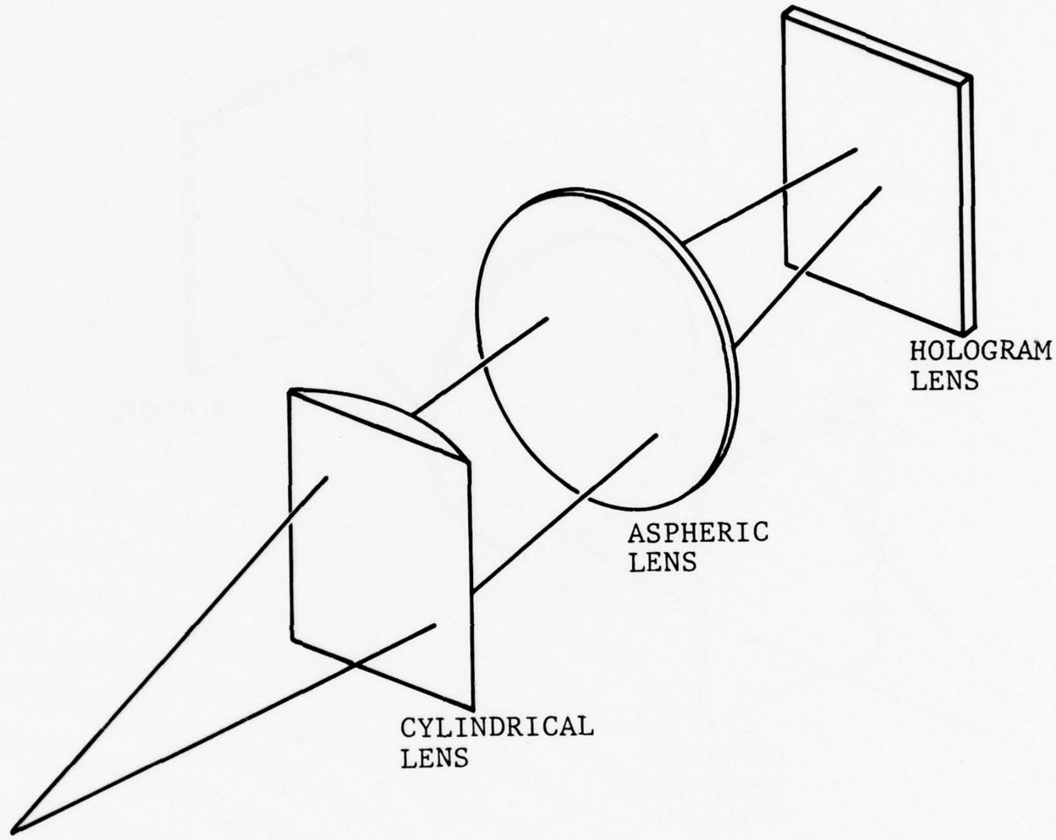

FIGURE 22. GENERATION OF ARBITRARY PHASE WAVEFRONT WITH CONVENTIONAL OPTICS

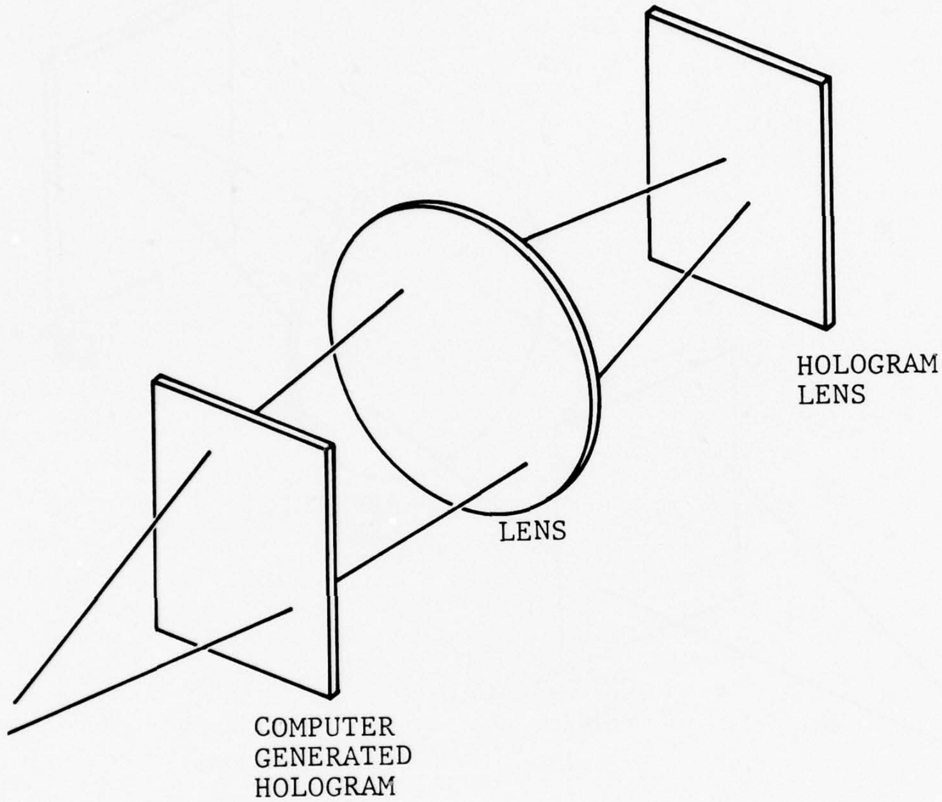

FIGURE 23. GENERATION OF ARBITRARY PHASE WAVEFRONT WITH HOLOGRAPHIC OPTICS

5
CONCLUSIONS

This was a preliminary design effort to determine the feasibility of utilizing holographic optics in a one-tube, two-eye goggle. The goggle requirements place a severe burden on the hologram performance, requiring formation of an image with reasonable quality over a wide field-of-view and with high diffraction efficiency. It is clear that satisfying the goggle requirements pushes the state-of-the-art of hologram optical element design techniques.

Of the systems analyzed, the Two Lens Design (system nine) showed the greatest immediate promise. As might be expected, it is the most complex system we analyzed, including holograms on curved substrates and two conventional lenses. Although the performance is marginal in some respects, the system does show promise, and represents a vast improvement over the initial design.

The Fiber-Optics Twist Design also shows promise but probably requires new techniques to realize acceptable performance. These techniques are the development of analytical and experimental procedures for generating construction wavefronts with arbitrary phase. The most attractive feature of the Fiber-Optic Twist Design is its simplicity, relying on only two hologram lenses.

Although the fiber-optics twist has been retained, only one twist will be required in the one-tube system, and its weight will be offset in part by the lack of any conventional lens elements (between the twist and the user's eye).

6 RECOMMENDATIONS

Further design investigations are recommended to provide a definitive answer concerning the feasibility of a goggle design utilizing holographic optics. It is expected that the last two designs described in Section 3 would provide a good starting point for further investigations. Areas of particular interest include addition of a pre-image lens, consideration of a plane-wave input, assumption of arbitrary phase wavefronts for the hologram construction, and investigation of available phosphors and the impact of their bandwidths on system performance.

6.1 PRE-IMAGE LENS GEOMETRY

This geometry adds a conventional or holographic lens between the phosphor screen and the first holographic lens. The major objective of this approach is to increase the amount of phosphor light that reaches the first holographic lens. The reflective geometry of the current design requires that the phosphor screen be adequately separated from the hologram lens to permit the diffracted rays to reach the secondary holographic lenses. Although the image inversion between the two hologram elements reduces the separation requirement, we recommend exploring the possibility of further decreasing the effective separation by placing a lens near the phosphor screen. This lens is called a pre-image lens because it occurs before the first image is formed by the system. It may help to lower aberrations by reducing the requirements on the first holographic lens, which in the current design requires a short focal length. The lens may provide further reduction of system aberrations, if necessary, by providing for early correction of aberrations within the system; it is desirable, however, to keep the lens relatively simple and lightweight.

6.2 PLANE-WAVE INPUT ILLUMINATION

This approach to the system illumination assumes that the input to the first element is strongly directional, approaching a plane wave rather than point scatterers from the phosphor screen. Such an input might be derived, for example, from a (diode) laser-illuminated transducer at the output of the image intensifier tube. The laser-illuminated transducer offers an advantage in two respects: first, most or all of the light from the transducer would reach the first element in the optical train and second, by adjusting the laser power, it should be possible to vary the image brightness without changing the intensifier tube parameters. The plane wave input provides additional flexibility by making the two holographic elements matched in focal power and angle with plane waves only as input and output of the holographic portion of the system. We would expect reduced aberrations by achieving a more favorable bending factor without substantial violation of the Bragg conditions of the two hologram lenses. Furthermore, the symmetry of the holographic portion of the system suggests that a design might be realized in which there is considerable aberration compensation by the two holograms themselves.

6.3 ARBITRARY PHASE WAVEFRONTS

As we discussed in Section 4, construction of one or both hologram lenses with arbitrary phase wavefronts may allow the realization of an all-holographic design. Indeed, development of arbitrary phase wavefront analysis and implementation (perhaps through computer generated holograms) appears to be the next major step in the development of holographic optics. Arbitrary phase wavefronts should increase the general usefulness and applicability of holographic lenses to a variety of tasks.

6.4 INPUT ILLUMINATION

Because of the preliminary nature of this investigation, little attention was given to the nature of the input illumination. Since holograms are rather sensitive to changes in wavelength, the bandwidth of the input illumination should be considered in detail in any further investigations. Here we would recommend an integrated systems approach in which the phosphor is selected to meet, in an optimum fashion, the requirements and constraints of the overall system.

7
APPENDIX: HOLOGRAM ANALYSIS

The appendix serves to give a brief description of the hologram geometry and analysis procedures used in the Holographic Optics Analysis and Design programs. Figure 24 shows the pertinent geometry used in the hologram analysis. The figure is drawn with respect to an arbitrary point source Q situated in front of the hologram, which is positioned in the x-y plane. The distance from Q to the center of the hologram is R_q, and is positive if the point Q lies on the +z side of the hologram, and negative if Q lies on the -z side of the hologram. The projection of the line R_q onto the x-z plane forms an angle α_q with respect to the y-z plane. The angle α_q is measured with respect to the positive z portion of the y-z plane, and is positive when a rotation from the y-z plane to the point Q corresponds to the direction of rotation of a right-handed screw advancing in the +y direction. (The α_q shown in Figure 24 is positive.) Similarly the projection of the line R_q onto the y-z plane forms an angle β_q with respect to the x-y plane. The point Q in x, y, z space can be defined with respect to the hologram surface by three parameters R_q, α_q and β_q, or x_q, y_q and z_q. In terms of the construction and reconstruction geometries, the point Q is denoted by subscripts O, R, C and

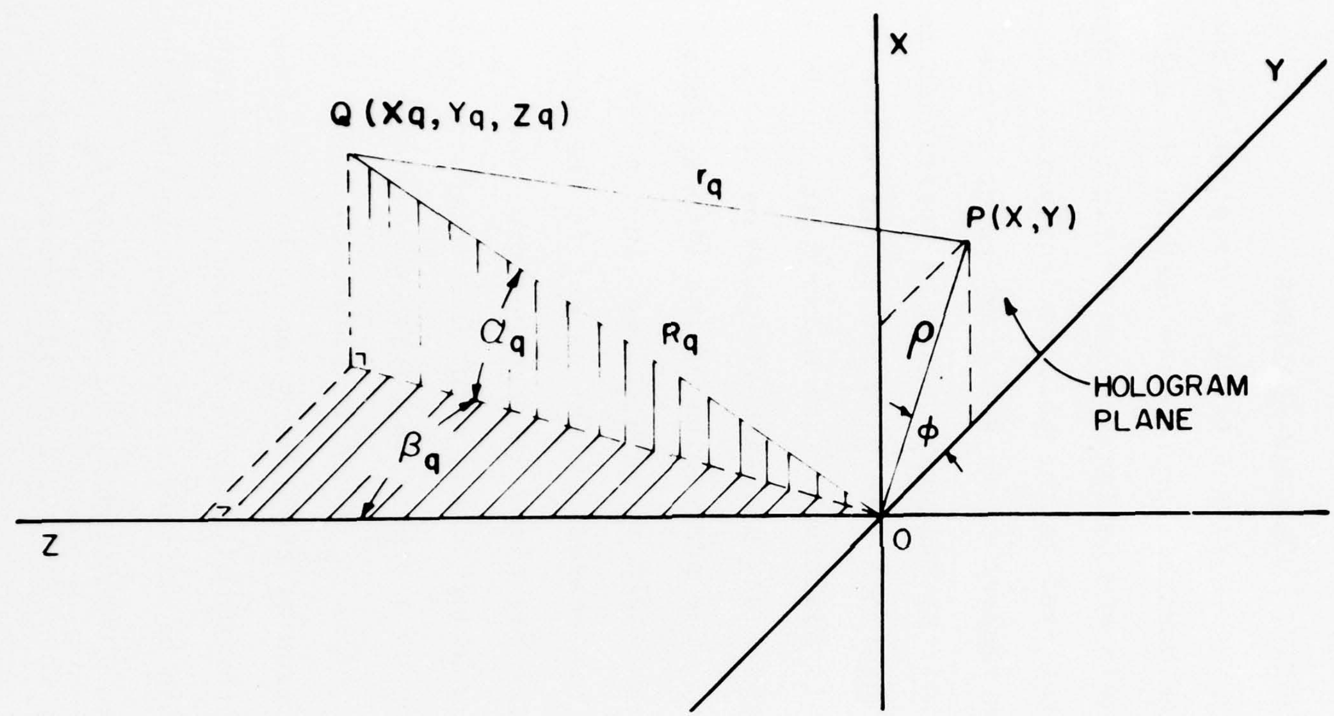

FIGURE 24. COORDINATE GEOMETRY OF AN ARBITRARY POINT SOURCE q AT x_q, y_q, z_q SITUATED IN x, y, z SPACE IN FRONT OF A HOLOGRAM IN THE x-y PLANE

I corresponding to object, reference, reconstruction, and image beams, respectively.

Some of the parameters involved in simulating a hologram are shown in Figure 25. Two point sources are used to construct the hologram; the reference and object sources are indicated by R and O, respectively. The variables which describe the location of the point sources are R, α, and β, or x, y, and z; each has subscripts appropriate to the source. The hologram is in the xy-plane and has the dimensions x_M, y_M, and D. The media on either side of the hologram may have different indexes-of-refraction, and we may specify the index of the hologram medium before and after processing. Surface curvature is specified at the vertex (in our analyses, the intersection of the surface with the z-axis) by the parameter CV, the reciprocal of the radius of curvature.

The reconstruction geometry is shown in Fig. 26. The sources of interest are C for reconstruction and I for the image. There may be different indexes-of-refraction on either side of the hologram. The point sources are again described with aid of α, β, and R, or x, y, and z. In addition, the hologram may be changed in thickness by the magnification factor M_z. The programs also incorporate the thick-media theory of Kogelnik[4], by which one can analyze the effects of the material on hologram ray efficiencies.

The programs are of greater utility when multiple elements are incorporated as illustrated in Fig. 27. Location

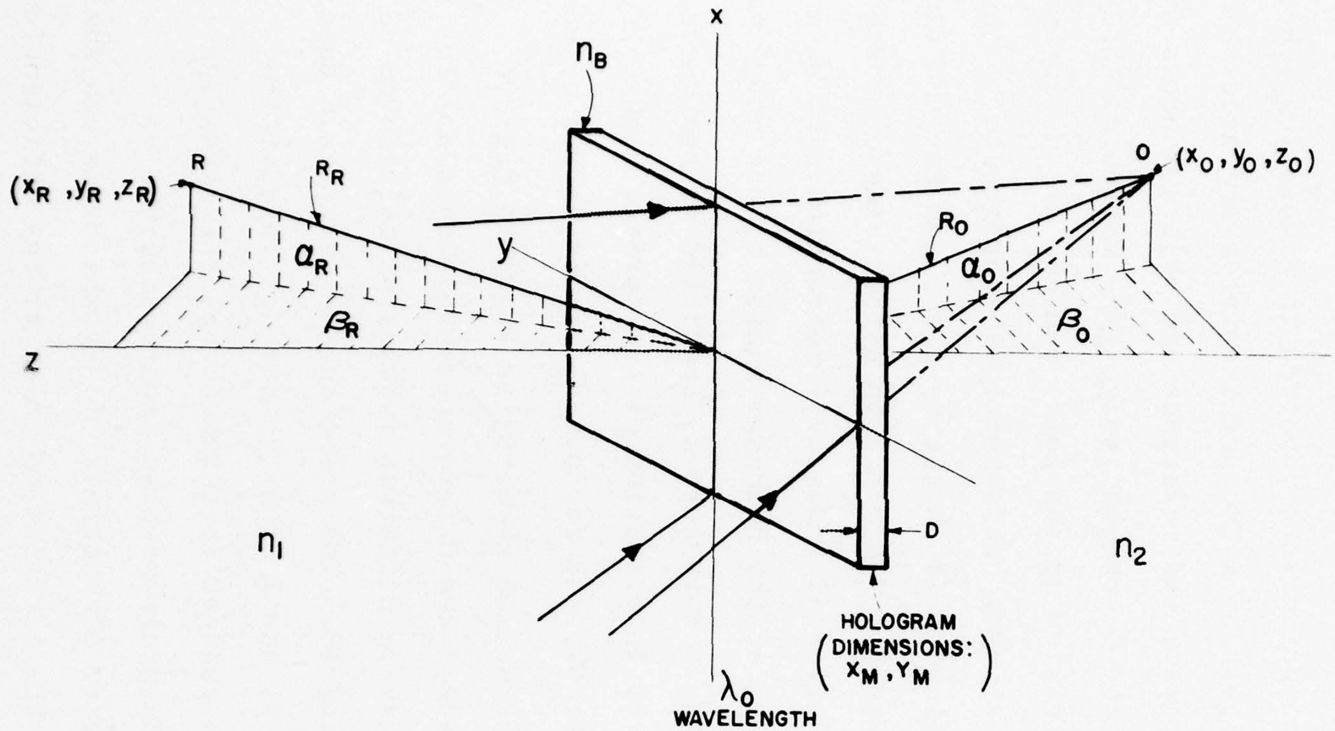

FIGURE 25. HOLOGRAM RECORDING PARAMETERS AND GEOMETRY

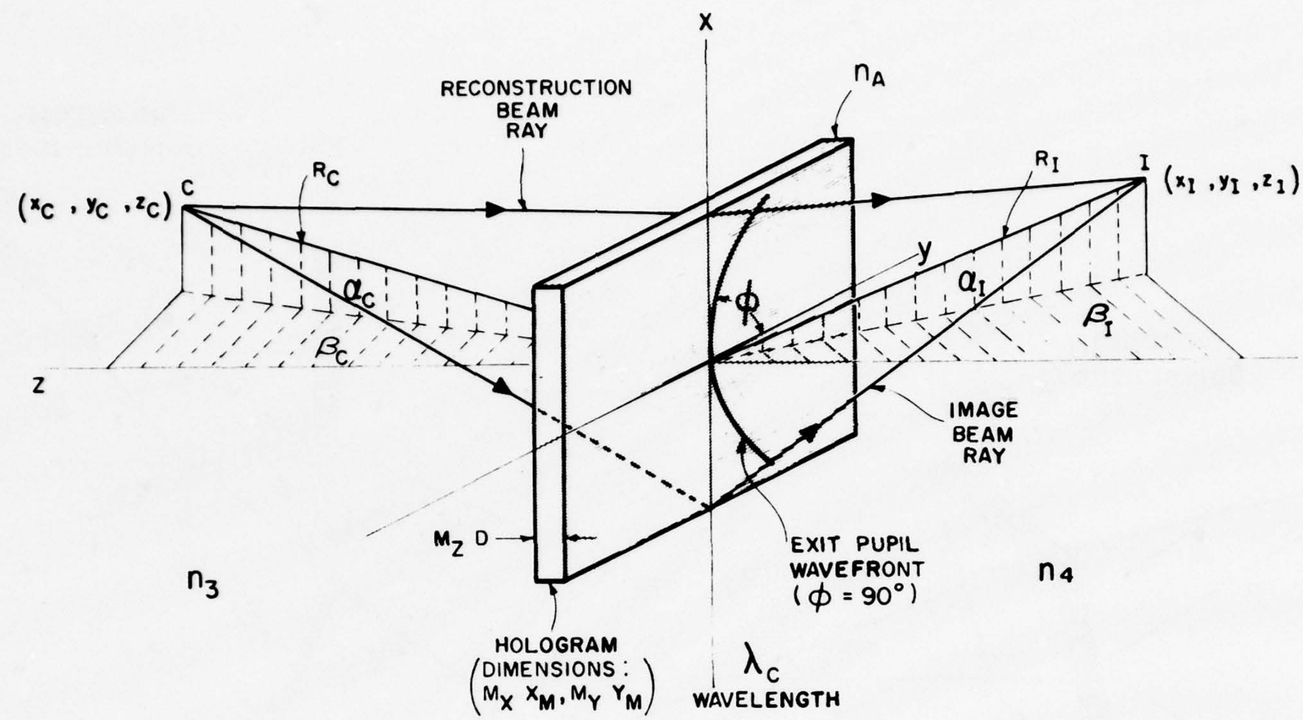

FIGURE 26. HOLOGRAM RECONSTRUCTION PARAMETERS AND GEOMETRY

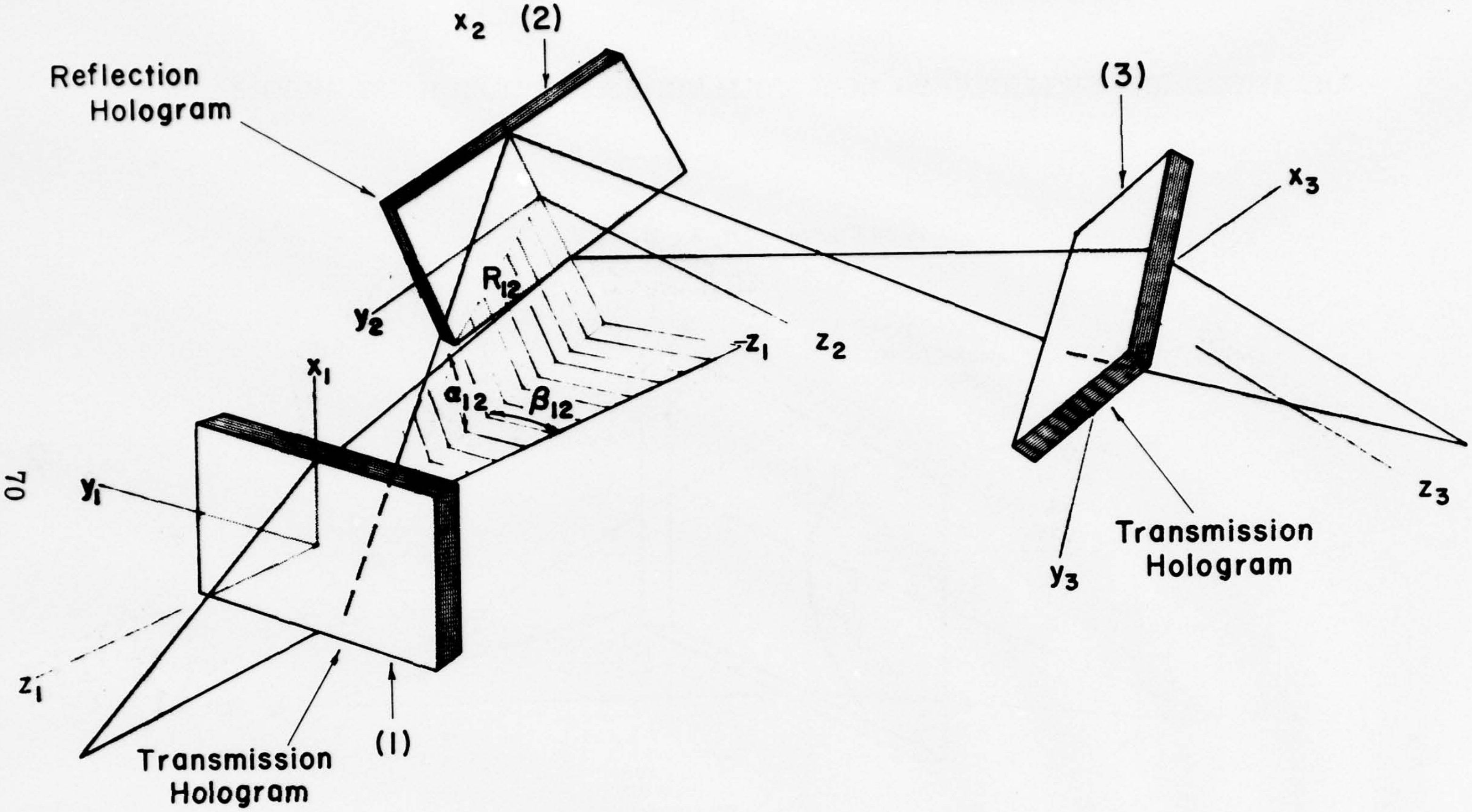

FIGURE 27. MULTIPLE HOLOGRAM ELEMENT GEOMETRY

and orientation of one hologram with respect to another is described by six variables. Three involve the description of the center of the hologram, n + 1, with respect to the hologram, n, using variables $\alpha_{n,n+1}$, $\beta_{n,n+1}$, and $R_{n,n+1}$. In addition, the hologram, n, may be rotated about Euler angles α_n, β_n, and γ_n to provide the full six degrees of freedom. Holograms which may be treated in the ray tracing programs include reflection and transmission types that may be either forward or backward illuminated. In addition, the ray-tracing programs may be extended to incorporate curved-surface elements; shown in Fig. 28 is an illustration corresponding to Fig. 27. The surfaces may be spherical, parabolic, hyperbolic, ellipsoidal, toroidal, or aspheric. The holograms may be reconstructed in any order, $\pm n$ and 0 (except for the thick media analysis, which currently is limited to the +1 order). Furthermore, the holograms may be of the forced reflection type; this mode permits the simulation of holograms made on a surface-relief material such as photoresist coated with a highly reflective material such as aluminum.

Conventional optics components that can be analyzed include lenses and mirrors with surfaces having the same generality as discussed above. Figure 28 illustrates a toric index of refraction surface from media n_1 to n_2. The second surface, which is a reflection hologram, has a conic shape.

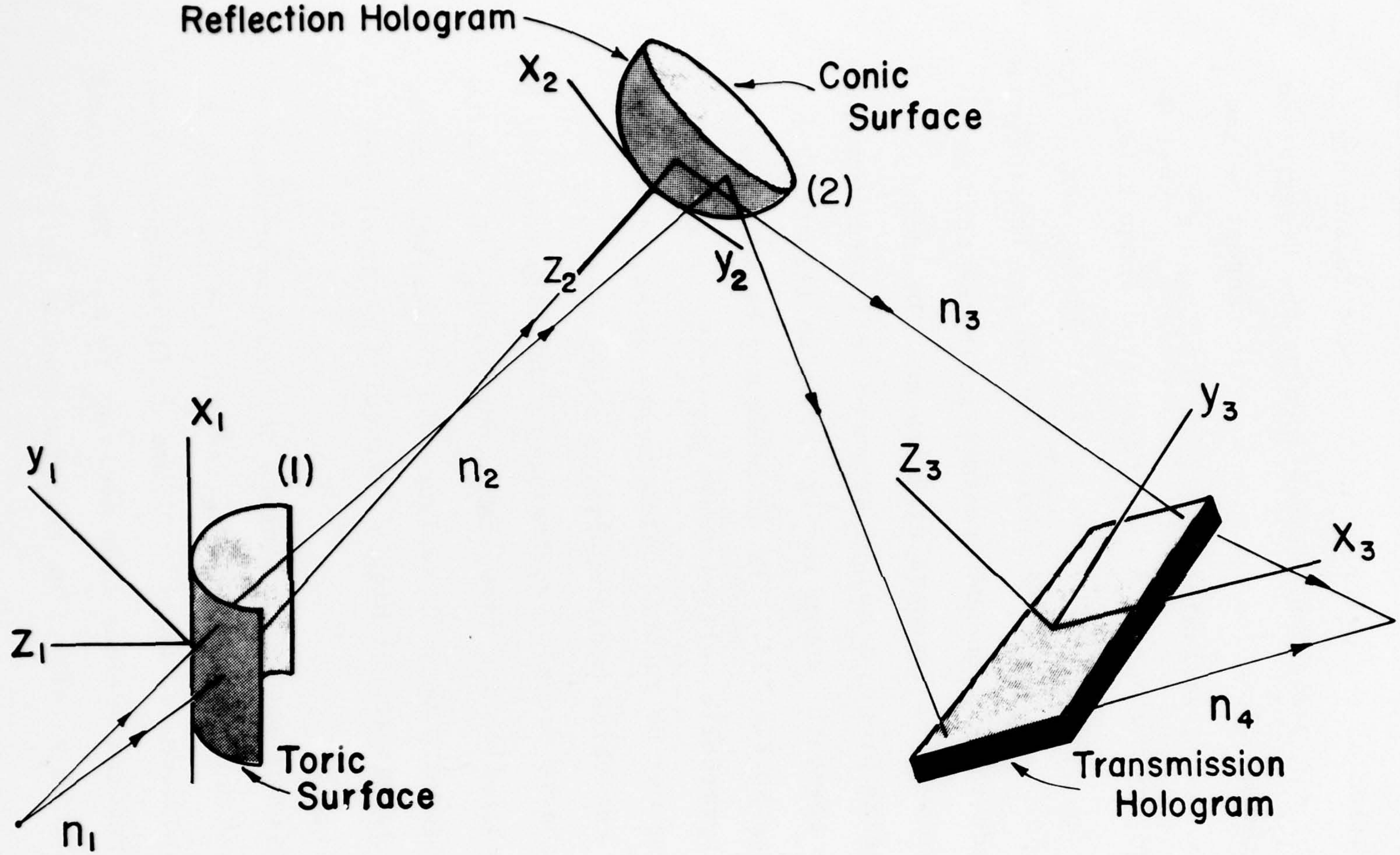

FIGURE 28. GENERAL HOLOGRAM AND OPTICAL SYSTEM GEOMETRY

The last, which is a transmission hologram, is a degenerate spheric, i.e., a plane surface.

The utility of these programs has been greatly enhanced by incorporating techniques for optimizing a given geometry to a particular level of performance. This extension is included in the optimization programs diagrammed in Fig. 29. These routines essentially serve as a driving program for the general ray-tracing programs described in the previous paragraphs. The programs have been designed with as much flexibility as possible: the input data stream allows the designer to choose from a host of options. The central core of the programs consists of the optimization-method library and merit-function library. Each library may be accessed, via the input, independently of the other. We can also construct a set of independent, but sequential, searches that operate on different variables in the same holographic system. For example, one might want to optimize a set of five variables for a given initial system for 50 given interactions through a given optimization technique. On the next pass it is possible to take the best resulting system from the last optimization results and operate on that system with a different set of variables, optimization methods, and merit functions. This can all occur within one set of input data to the program. The input can be structured so that the designer has access to any variable in the hologram system and may vary these over

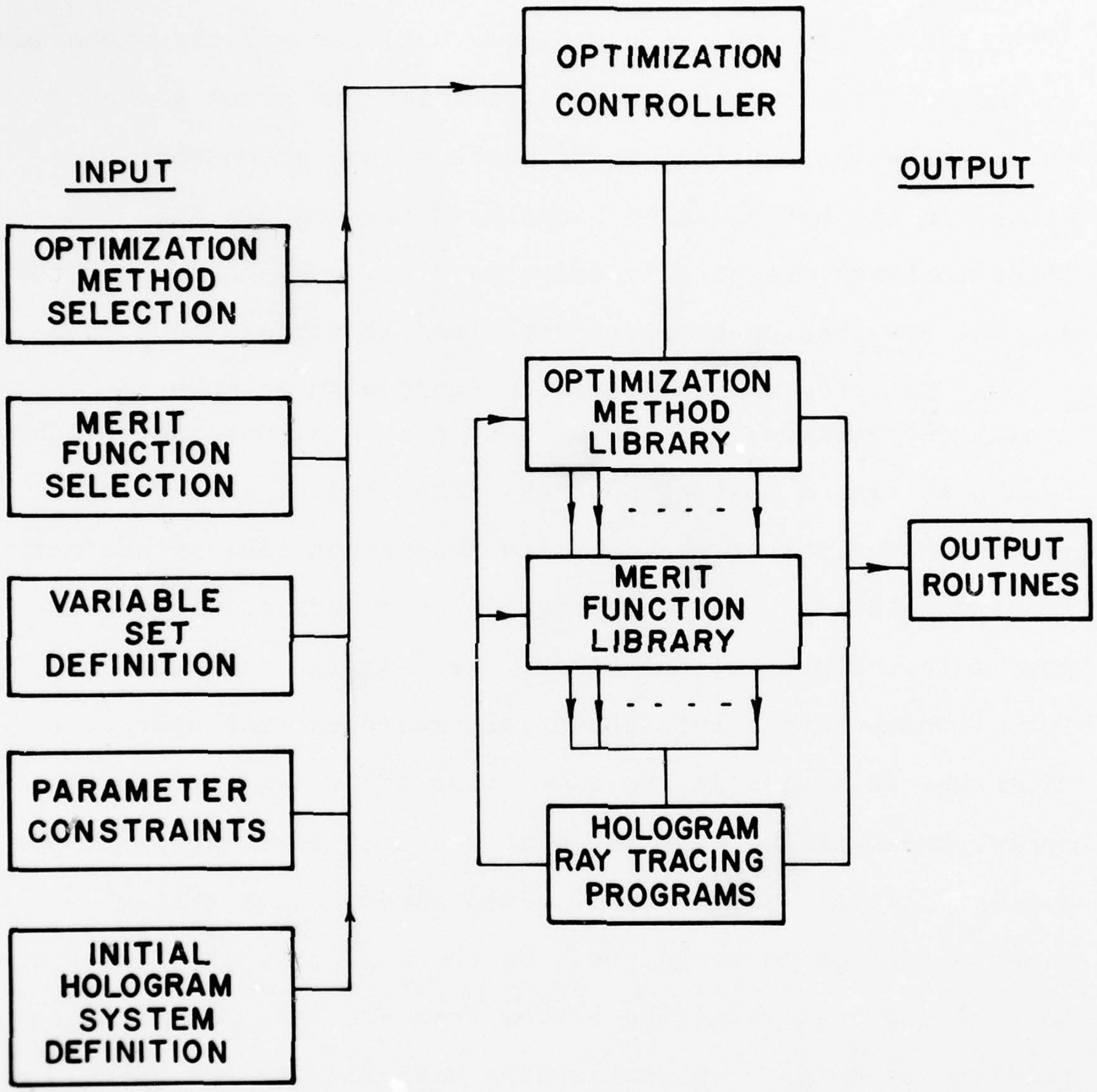

FIGURE 29. OPTIMIZATION PROGRAMS FOR HOLOGRAPHIC OPTICAL ELEMENTS

whatever limits are necessary. The merit functions are implemented in small subprograms, with the numerical results of ray-tracing programs used as inputs. The value of the merit function is then determined in the subprogram. These merit functions can be easily modified to include practically any mathematical function of interest to the designer.

A typical optimization run begins with the designer defining an initial hologram system, which is evaluated by the ray-tracing programs and the merit-function value is determined for this system. The designer also selects the parameter constraints such as reconstruction-wavelength band or reconstruction-angle variation. In addition, he selects not only the set of variables to be modified and their range, but also the merit function and optimization method. Each of these library components may access the variables without any *a priori* knowledge about or constraints on the properties of the variables. Hence, optimization programs are essentially independent of variables. This optimization program, in conjunction with the general multiple-element ray-tracing programs, provides a very powerful and flexible tool for the analysis of holographic optic systems.

REFERENCES

1. E. B. Champagne, "A Qualitative and Quantitative Study of Holographic Imaging," (unpublished PhD dissertation), Ohio State University, Columbus, 1967 (University Microfilms No. 67-10876).

2. J. N. Latta, "Computer-Based Analysis of Holography," Ph.D. Thesis, University of Kansas, Lawrence, Kansas, December 1970 (U. Microfilm No. 71-27, 168).

3. J. N. Latta, "Computer-Based Analysis of Hologram Imagery and Aberrations," Appl. Optics, 10, pp. 599-618, March 1971.

4. J. N. Latta, "Computer-Based Analysis of Holography Using Ray Tracing," Applied Optics, Vol. 10, No. 12, pp. 2698-2710, December 1971.

5. J. N. Latta and R. C. Fairchild, "New Developments in the Design of Holographic Optics," Proceedings of the Seminar on Applications of Geometrical Optics (ed. by W. J. Smith), Society of Photo-Optical Instrumentation Engineers, Redondo Beach, 1973, pp. 107-126.

6. H. Kogelnik, in Proceedings of Symposium on Modern Optics, J. Fox, Ed. (Polytechnic Press, Brooklyn, N. Y., 1967), pp. 605-617.

7. W. S. Colburn, R. G. Zech, and L. M. Ralston, "Holographic Optical Elements," Technical Report, AFAL-TR72-409, (1973).

8. J. N. Latta, "Analysis of Multiple Hologram Optical Elements with Low Dispersion and Low Aberrations", Appl. Opt. 11, pp. 1686-1696, August 1972.

9. H. W. Rose, "Holographic Lens Systems," Ph.D. Thesis, Dept. of Electrical Engrg. Ohio State University, Columbus, Ohio, 1972.

10. R. H. Katyl, "Compensating Optical Systems, Part 1: Broadband Holographic Reconstruction", Appl. Opt. 11, pp. 1241-1247, May 1972.

REFERENCES (Continued)

11. W. S. Colburn, ARPA Quarterly Technical Report on Evaluation of Hologram Optical Elements, Report No. 194500-4-T, Environmental Research Institute of Michigan, Ann Arbor, February 1974.

12. W. S. Colburn and B. J. Chang "Evaluation of Hologram Optical Elements", ARPA Quarterly Technical Report, Report No. 194500-5-T, Environmental Research Institute of Michigan, August 1974.

13. D.C. Chu, J.R. Fienup, and J.W. Goodman, "Multiemulsion On-Axis Computer Generated Hologram", Appl. Opt. 12, pp. 1386-8, July 1973.